Long-term variability of aerosol optical thickness in Eastern Europe over 2001-2014 according to the measurements at the Moscow MSU MO AERONET site with additional cloud and NO2 correction

N.Y. Chubarova, A.A. Poliukhov, I.D. Gorlova

Moscow State University, Faculty of Geography, Russia, 119991

Correspondence to: N.Y.Chubarova (chubarova@geogr.msu.ru)

Abstract

The aerosol properties of the atmosphere were obtained within the framework of the AERONET program at the Moscow State University Meteorological Observatory (Moscow MSU MO) over 2001-2014 period. The quality data control has revealed the necessity of their additional cloud and NO_2 correction. The application of cloud correction according to hourly visual cloud observations provides a decrease in monthly averages of aerosol optical thickness (AOT) at 500 nm of up to 0.03 compared with the standard dataset. We also show that the additional NO_2 correction of the AERONET version 2 data is needed in large megalopolis, like Moscow, with 12 million residents and the NO_x emission rates of about 100 $ktyr^{-1}$. According to the developed method we estimated monthly mean NO_2 content, which provides an additional decrease of 0.01 for AOT at 340nm, and of about 0.015 – for AOT at 380 and 440nm. The ratios of NO_2 optical thickness to AOT at 380nm and 440nm are about 5-6% in summer and reach 15-20% in winter when both factors have similar effects on UV irradiance. Seasonal cycle of AOT at 500nm is characterized by a noticeable summer and spring maxima, and minimum in winter conditions, changing from 0.08 in December and January up to 0.3 in August. The application of the additional cloud correction removes a local AOT maximum in February, and lowered the December artificial high AOT values. The pronounced negative AOT trends of about -1–5%yr^{-1} have been obtained for most months, which could be attributed to the negative trends in emissions (E) of different aerosol precursors of about 135 $Ggyr^{-2}$ in E_{SOx}, 54 $Ggyr^{-2}$ in E_{NMVOC}, and slight negative changes in NO_x over European territory of Russia. No influence of natural factors on temporal AOT variations has been revealed.

1 Introduction

Atmospheric aerosols are among the most important factors influencing net radiation at the top and at the bottom of the atmosphere and, therefore, affecting the whole climate system (IPCC, 2013). However, still there is not enough information about their optical properties over different geographical regions. The knowledge of long-term variations of aerosol optical thickness can significantly affect the assessment of climate change, and at the same time can be an indicator of changes in emissions of aerosol precursors (Tegen et al., 1997).

Different aerosol characteristics are possible to obtain from satellite instruments, i.e. Advanced Very High Resolution Radiometer (AVHRR), Moderate Resolution Imaging Spectroradiometer (MODIS), Advanced Along-Track Scanning Radiometer (AATSR), medium-spectral resolution, imaging spectrometer MERIS, Polarization and Directionality of the Earth's Reflectances (POLDER), Ozone Monitoring Instrument (OMI), Cloud-Aerosol Lidar and Infrared Pathfinder Satellite Observations (CALIPSO), Sea-Viewing Wide Field-of-View Sensor (SeaWiFs), Multi-angle Imaging Spectroradiometer (MISR), etc. (IPCC, 2013). However, still the ground-based measurements are characterized by the best accuracy and serve as a reference for comparisons. Ground-based aerosol networks such as Global Atmosphere Watch Precision Filter Radiometers (GAW-PFR), AErosol RObotic NETwork (AERONET), observation network SKYNET, Siberian system for aerosol research (SibRad), Micro-Pulse Lidar System (MPLNET) provide high quality aerosol measurements (http://www.wmo.int/pages/prog/arep/gaw/aerosol.html). Aerosol Robotic Network (AERONET) (http://aeronet.gsfc.nasa.gov/) has been in operation since the middle of 1990s (Holben et al., 1998) with currently more than 400 sites continuously working all over the world. AERONET is equipped with CIMEL sun/sky photometers, which provide accurate measurements of direct solar irradiance and multi-angle sky radiance from UV to near-infrared spectral region for evaluating aerosol optical thickness and many other inversion products including size distribution, effective radii, aerosol phase function, and different optical and radiative aerosol properties – refractive index, single scattering albedo, asymmetry factor, etc. (Dubovik and King, 2000).

In order to eliminate the cases, which are degraded by cloud-contamination a special cloud-screening procedure has been used in the AERONET algorithm (Smirnov et al., 2000). In addition, in the second version of the AERONET dataset (Holben et al., 2006) the correction on several optically effective trace gases (NO_2, O_3, CO_2, H_20, CH_4) has been applied for the measurements in different channels.

The continuous aerosol measurements at the Moscow State University Meteorological Observatory (Moscow MSU MO) within the AERONET program have been in operation since August 2001. These records provide a reliable dataset for studying long-term variability of aerosol properties in the Eastern

Europe, where the aerosol network is sparse. In addition, the auxiliary hourly cloud visual observations and measurements of different trace gases at the MSU MO over the whole period of observations enable us the data for testing the existing AERONET algorithms and improving the quality of the aerosol dataset. This is important since one can see still the effects of residual thin homogeneous upper layer cloud contamination in aerosol retrievals even in the final AERONET dataset (O'Neill et al., 2003, Uliumdjieva et al., 2005, Chew et al., 2011, Huang et al., 2012). One of the tasks of this paper is to demonstrate the effects of the additional cloud-screening procedure and NO_2 correction on evaluation of aerosol climatology in Moscow. Using the revised aerosol dataset we studied the seasonal features and long-term aerosol optical thickness (AOT) variability over the 2001-2014 period. We also tried to find explanation of the obtained AOT trends in Moscow and showed the possible natural and human induced effects on its character.

2 Data description

The procedure of aerosol measurements by CIMEL AERONET sun/sky photometer and the inversion algorithms were described in numerous publications (http://aeronet.gsfc.nasa.gov/new_web/publications.html). MSU MO site utilizes the 1.2° full field of view CIMEL CE318 sun and sky photometer. The direct solar radiation measurements in the 340, 380, 440, 500, 675, 870, and 1020 nm channels are used for aerosol optical thickness retrievals; the measurements in the 940 nm channel are used for the evaluation of water vapor content W. In addition, direct spectral irradiance measurements are applied for the retrievals of fine and coarse aerosol modes according to the spectral deconvolution algorithm [O'Neill et al., 2001, 2003]. Both sun and sky-radiance in the channels 440, 675, 870 and 1020 nm are utilized in the inversion algorithm developed by Dubovik and King [2000], which provides several important aerosol products (volume size distribution, refractive index, single scattering albedo, phase function, etc.). The uncertainty of aerosol optical thickness measurements does not exceed 0.01 in visible range and 0.02 - in UV spectral range (Eck et al., 1999, Holben et al., 2001). However, there are some important but still not fully resolved problems, which include testing and further improvement of cloud-screening algorithm and the additional correction on NO_2 in large megalopolis like Moscow. For the improvement of these procedures, in addition, we used visual cloud observations with 1 hour resolution. The uncertainty of visual cloud amount measurements is about 1 or 2 cloud fraction (in tenth) according to (Handbook, 1989), however, the conditions with overcast or zero cloudiness are observed accurately by any observer. In addition, the dataset of hourly solar disk condition observations, which are performed simultaneously with cloud observations, was used in the analysis. This is a standard type of observations at the actinometrical stations in Russia. Using this characteristic we can distinct the conditions, when solar disk (SD) is free from clouds, or when SD is

obscured by thin clouds (shadows can be seen at ground), or when SD can be seen but there are no shadows at ground, or when SD can not be seen due to relatively high cloud optical thickness. These SD conditions are noted with "2", "1", "0" and "P" marks, respectively.

For quantifying the NO_2 content, we used in-situ long-term 1 minute resolution measurements of NO_2 concentrations by APNA-360, Horiba Inc. (Elanski et al., 2007) at the Moscow MSU MO at the altitude of about 3.5 meters from ground since 2002. The NO_2 data were used as the input parameters in the developed algorithm described in (Chubarova et al., 2009) for the independent evaluation of NO_2 content in the low troposphere over urban Moscow area. The details of the methods and the results are discussed below in the next section. In addition, we used some standard meteorological and radiative measurements at the Meteorological Observatory of Moscow State University which are described directly in the text.

3 Results

3.1 The effects of the additional cloud-screening and NO_2 correction on aerosol climatology

3.1.1 Additional cloud-screening procedure and its effect on aerosol climatology

Since the aerosol measurements are carried out in automatic regime, a special cloud-screening procedure was developed for an automatic removal of cloud contaminating aerosol measurements (Smirnov et al., 2000). In the standard AERONET algorithm the data, which successfully pass the cloud screening procedure, are assigned to the level 1.5. After the second calibration and some additional visual checks the data are assigned to the final level 2.0. However, sometimes even the final dataset could "suffer" from the effects of thin homogeneous upper cloudiness contamination (O'Neill et al., 2003). As was mentioned in this paper "the strategy of the AERONET cloud screening was liberal; to interfere as little as possible with coarse mode events such as dust incursions and thus to accept the inevitability of some thin homogeneous cloud data, being admitted into the database." Hence, the question remains, how important can be this effect. Will it significantly affect the aerosol climatology?

For evaluating the upper layer cloud contamination in the AERONET dataset different approaches are used. In the recent studies the ground-based MPLNET, as well as satellite CALIPSO and MODIS datasets were used for evaluating the cirrus AOT contamination (Chew et al., 2011, Huang et al., 2012). According to MPLNET data the AOT bias due to unscreened cirrus cloud presence is about 0.03-0.06 with the occurrence of 23-34% depending on the method of the estimation over the tropical region in Singapore (Chew et al., 2011). Huang et al. (2012) evaluated the susceptibility percentage of AERONET level 2.0 AOT retrievals to cirrus contamination using different types of measurements. According to

MPLNET cirrus flags this value varied from zero to ~4%, according to the collocated Calipso cirrus flags - from 1% to 33%, and according to the MODIS cirrus flags - from 0.4% to 18% changing significantly over the globe due to the different occurrence of cirrus clouds. However, satellites have relatively low overpass frequency over AERONET sites - one-two time a day – for MODIS, and 16-day repeating cycle - for CALIPSO (Huang et al., 2012). The MPLNET application for cirrus flags has the problem with viewing geometry difference between the sunphotometer and the MPL. In addition, the MPL signals are extremely weak at the altitudes H> 10 km, where cirrus clouds may be observed. It was also mentioned in (Huang et al., 2012) that the MPL noise level dramatically increases during daytime especially at noon, when there are most favourable conditions for AERONET-MPLNET matchup from the point of view of the closeness of viewing geometries.

The influence of the cloud contamination on aerosol properties was also discussed in (Uliumdzhieva et al., 2005) for Moscow conditions. In this paper the application of the standard cloud visual observations as an additional cloud-screening filter was proposed. We used one-hour resolution cloud observations for additional filtering of quasi-simultaneous Cimel observations at the same site. The application of cloud filter means the elimination of all AOT measurements for the entire hour interval. We showed there that the existing standard cloud-screening algorithm works perfectly, when aerosol measurements are contaminated by optically thin low layer cloudiness, which is characterized by large triplet variations. These variations are used as a parameter in the standard cloud-screening algorithm developed by Smirnov et al. (2000). However, if the cloud blocking the Sun is thin and uniform, the triplet variation can be small and the contaminated AOT measurements pass through the filter. Mainly the cirrus clouds are characterized by these properties. However, in general, according to the International Cloud Atlas (1987) other types of clouds may be also characterized by these properties as well. They include different forms of Cirrostratus, and even Altostratus translucidus clouds, which relate to the middle cloud level. In this publication all types of the cloudiness, which can induce the potential contamination of AOT will be combined under the term “upper cloudiness”.

Since low cloudiness is effectively filtered out by the standard cloud-screening algorithm we proposed to apply simple total cloud amount (NA) filter, which is sensitive to the existence of upper cloudiness. In this context NA value (together with the application of standard cloud-screening procedure) provides the information about the potential existence of high and middle layer cloudiness, since the standard AERONET cloud-screening algorithm successfully removes the cases contaminated by low level clouds or the cases with strong signal variations. However, the application of different NA thresholds may provide the different samples and as a result, different statistics. As an example, in Fig.1 we demonstrate the effects of utilizing the different additional NA filters for AOT at 500nm (AOT500) and Angstrom exponent (α) datasets for the central months of the seasons. One can see a similar tendency

of the AOT decrease in all seasons after removing the cases with the threshold of NA<9, which includes the conditions with almost total cloud amount of NA= 9-10. Additional testing on solar disk conditions has revealed that all eliminated cases in this sample belong to the situations, when solar disk was covered by clouds (SD=1 or SD=0). In April after eliminating the almost overcast cloud conditions with NA<9 threshold there is no further changes in AOT500 samples with more strict NA cloud threshold. At the same time the sample is dramatically (more than twice) reduced (from 229 to 113 in NA<3 sample). In July we also see a slight decrease in AOT500 in the NA<9 sample and, in addition, a significant growth of Angstrom exponent. Note, that in July and October we see even a slight increase in the AOT500 for almost clear sky conditions (the sample with NA<3). In January there is a pronounced decrease in AOT500 with reducing cloud amount. The lowest AOT500 values and largest Angstrom exponent are observed in the NA<3 sample. The application of the 24-hour Hybrid Single-Particle Lagrangian Integrated Trajectory (HYSPLIT) NOAA model backward trajectory analysis (Draxler and Hess, 1998) for all the cases in January has revealed for the NA<3 sample the prevalence of the northern (North-West, North, North-East) advection (80% of cases) characterized by low AOT (Chubarova, 2009), compared with 40% of cases for partially cloudy conditions (3<NA<9). At the confidence level of P=80% several of these dependencies are statistically significant (see the error bars in Fig.1).

Balancing between the substantial decrease in case number and the accuracy of the retrievals of aerosol properties we showed that the best results were obtained when the cases with $N_{total.}$<9 during March-October period with almost overcast cloudiness and cloud contaminated solar disk conditions data were removed. For November –February conditions the filter threshold is more strict (N_{total}<6) since solar elevation in Moscow is low (h_{noon}<25°) at this time and a well-known effect of significant visual cloud amount increase towards the horizon plays a vital role. Smaller cloud threshold during winter time may induce filtering out so called "good" AOT cases. The additional analysis of solar disk conditions has revealed only 12 cases from 2521 cases (about 0.5%), which were not contaminated by clouds (SD=2) and were incorrectly removed from the sample. All of them were observed in February (18.02.2011 – 4 cases, 3.02.2003- 5 cases, 11/02/2007 - 3 cases). However, even these three days are presented in the final sample since during these days there were other sun photometer measurements at smaller NA.

In addition, we analyzed the 1-minute resolution direct solar measurements with the standard Russian actinometer (WMO, 1986) for studying the possibility of AERONET direct solar irradiance observations in cloud gaps,. These data were used for estimating the standard transparency coefficient at air mass m=2 according to (Evnevich, Savikovsky, 1988):

$$p_2 = \left(\frac{S_h}{1.367}\right)^{\frac{sinh+0.205}{1.41}}, \quad (1)$$

where S_h - is the measured value of direct shortwave irradiance, h - solar elevation.

The p_2 coefficient is widely used for assessing the variation of the transparency of the atmosphere (Ohvril et al., 2009). Using this equation we evaluated the integral optical thickness as $\tau = -\ln(p_2)$.

This characteristic was used as the indicator for the analysis of possible AERONET CIMEL sun photometer measurements in cloud gaps. The 1-minute resolution data provide us the time series to check whether CIMEL 15-minute resolution measurements can be observed in these cloud gap conditions. Since the duration of sunphotometer measurement is about 1 minute we can compare them with 1-minute resolution τ variations around the CIMEL observation. The condition with cloud gap should relate to the τ lowest optical thickness in the moment of CIMEL observations within a few minutes around. Note, that we used the τ data series only as an indicator of high frequency solar irradiance signal variations and we do not consider their absolute values.

For illustrating this phenomenon, Fig.2 presents the diurnal variations of 1- minute resolution τ, AERONET level 2.0 AOT500 and Angstrom exponent data series in conditions with cloud contamination during the two days – February 27th, 2005 and February 1st, 2006 with different cloud conditions. Weather conditions on February 27th, 2005 were characterized by the presence of Cirrus, Cirrocumulus and Altocumulus clouds. Solar disk was covered by thin clouds (SD=1), the (NA) cloud amount was equal to 10. We can see that on February 27th, 2005 AOT500 observations do not correspond to the smallest values of τ around, and, hence, there were no cloud gaps conditions during AOT500 measurements (Fig.2a). The similar results were obtained on February 1st, 2006, when during the entire day Cirrus clouds with NA=10 and NA=6 were observed (Fig.2b). The morning conditions were characterized by thin overcast cloudiness with NA=10, SD=1 and low AOT500. During the day the cloud amount decreased (NA=6) but we see the gradual increase in cloud optical thickness obscuring the Sun, which is in agreement with τ data series, and with the decrease in Angstrom exponent. Note, that even SD=0 conditions were observed after noon time. The τ time series with 1-minute resolution around AERONET AOT500 measurements do not demonstrate any local decrease, but just more uniform distribution. Of course, there can be cloud gap conditions during AERONET AOT measurements, however, on average, the cloud optical thickness contamination may induce much larger effect on aerosol climatology than removing of few "good" cases. By this example we also illustrate the necessity of the additional more strict cloud screening in winter with the threshold at least equal to NA=6.

Using this approach we obtained a revised dataset with additional visual cloud-screening over the whole 2001-2014 period of observations in Moscow. Figure 3a,b shows the absolute and relative differences between the standard monthly mean aerosol optical thickness at 500nm (AOT500) and additionally cloud-screened AOT500 values, as well as the differences in water vapor content, Angstrom exponent, and variation in day number over the whole period of measurements. One can see a substantial systematically overestimation of monthly mean aerosol optical thickness at 500nm in the standard

AERONET dataset up to 0.03 for several months. For all months (except September and November) the error is higher than 0.01, which corresponds to the uncertainty of AOT measurements (ε=0.01, depicted by the line in Fig. 3). In some years the monthly mean difference can even exceed 0.1 (for example, in February 2005 and October 2012). A detailed analysis was made to understand the reasons of these large discrepancies with the standard AERONET AOT dataset. Fig.4 shows the comparison between the standard daily mean AOT500 and Angstrom exponent data and their values after additional cloud filtering. In February 2005 additional cloud filtering provided full elimination of measurements during 03.02.2005 and 27.02.2005, which were characterized by smaller Angstrom exponent and extremely high AOT on 27/02/2005. According to the additional checks we found that all these cases were observed in solar disk conditions with SD=1 or SD=0. The additional cloud filtering also provides a slight increase in Angstrom exponent during the other days in February 2005, that also indirectly confirms the elimination of cloud-contaminated cases. In October 2012 the application of the additional cloud filter provided removal of high AOT500 values on 04/10/2012 due to the existence of overcast cloud conditions with SD=1 and SD=0. However, since the Angstrom exponent was not small the cloudiness was rather thin on 04/10/2012. During the other days in October the difference in both aerosol characteristics obtained before and after the additional cloud filtering was negligible.

Due to existing AOT seasonal change the relative difference in AOT500 has a noticeable minimum in summer (5%) and the increase up to 20-30% during winter months when the occurrence of upper cloudiness is high and AOT is low. There is also discernible underestimation of Angstrom exponent in the standard AERONET dataset due to the influence of close to neutral scattering on large cloud droplet, which contaminate AOT values which are used for the Angstrom exponent evaluation. The relative bias in Angstrom exponent has also some tendency towards higher underestimation (from -1-2% to -6%) in the standard product in cold period. Both positive AOT difference and negative Angstrom exponent difference clearly indicate the reliable elimination of cloud contaminated cases after the application of additional cloud filter. It is interesting that water vapor content W is also overestimated in cloud contaminated conditions up to 0.05-0.07 cm (or 15-20%) during winter months possibly due to the additional absorption by ice and water particles. However, there can be another reason for this phenomenon: the air convergence may create favorable conditions with higher relative humidity and water vapor content in the atmosphere, and, hence, the existence of clouds (see, for example, Jeong, Li, 2010). However, these processes should be studied further.

After the application of an additional cloud filter the day number significantly decreases (see Fig.3b): up to 7-20% during warm period, and 25-45% in cold period due to higher occurrence of overcast upper layer cloudiness and the application of more strict filter NA<6. Note, that small day number with aerosol observations in winter due to cloudy conditions results in large relative changes of

the removed day number even when only 1-2 days are removed from the initial statistics. These values are in a qualitative agreement with the cirrus susceptibility percentage tests of AERONET level 2.0 AOT retrievals against the CALIPSO vertical feature masks (Huang et al.,2012), but they differ from the similar assessments against Micro-Pulse Lidar data shown in the same paper. However, the application of the Micro-Pulse Lidar data for evaluating the cirrus cloud contamination over Tropical area (Chew et al., 2011) has revealed much higher susceptibility percentage (about 23-34%) of the AOT sample, which is in qualitative accordance with our data for winter months.

However, several recent studies indicated that clouds can have a real impact on AOT. These mechanisms of aerosol/cloud interaction include aerosol hygroscopic growth, increasing aerosol concentration due to air convergence, and new particles formation in the presence of clouds (Su et al., 2008, Jeong , Li, 2010, Eck et.al. 2012, Eck et.al. 2014). In addition to well known hygroscopic growth of particles there is a mechanism of the gas-to-particle conversion, which occurs more intensively in the aqueous phase in cloud droplets due to the oxidation of gases (SO_2, NOx, SOA) (Eck et al., 2014). Due to this mechanism in the presence of convective cloudiness the formation of new aerosol particles may observe providing higher aerosol loading during the periods with higher cloud amount in the vicinity of clouds (Eck et.al. (2014). The same mechanism also provides lower Angstrom exponent values.

Another mechanism of simultaneous variations in both aerosol and cloud amount is the changes in meteorology conditions, when, depending on advection and circulation features one can obtain synchronous changes in AOT and cloud amount, which do not interact with each other. A good example of this effect is the noticeable dependence of AOT and Angstrom exponent on various cloud filters for January. As discussed above, according to the results of 24-hour HYSPLIT backward trajectory analysis the collocated changes in AOT and cloud amount (value of cloud filter, see Fig.1) are likely observed due to the changes in advection. However, during warm period according to our long-term dataset we did not obtain the AOT-cloud amount dependence, except 100% contaminated cases when the NA<9 threshold filter has been applied. We should also mention that after applying this filter, which removes the data when solar disk was blocked by cloud, we do not remove any cases with particular convective cloudiness development, except those, which have been removed by the standard AERONET cloud-screening algorithm. However, it will be interesting to compare the results with the coming AERONET version 3 dataset, where a modification of standard cloud-screening algorithm will be applied to the data according to the method described in (Eck et al., 2014).

3.1.2 NO_2 correction algorithm and the effects of the revised NO_2 climatology on AOT estimations

The version 2 AERONET algorithm includes the correction on different trace gases content (http://aeronet.gsfc.nasa.gov/new_web/Documents/spectral_corrections_v2.pdf). Among them nitrogen dioxide (NO_2) has a significant absorption in UV and several visible channels, especially over the urban/industrial areas.

We should emphasize that Moscow is a large megalopolis with significant level of NO_x emission of about 100 $ktyr^{-1}$ (Ivanov et al., 2012). According to the data of Mosecomonitoring Agency the actual NO_2 surface concentrations in clean background conditions near Moscow are about 70% lower than those observed in Moscow (Report on the State of the Environment in Moscow, 2014). The spectral correction of aerosol optical thickness on NO_2 in the AERONET algorithm is made according to the SCIAMACHY climatology data over the 2003-2005 period (http://www.temis.nl/airpollution/no2.html) (Eskes et al.,2004). However, other studies have revealed much higher NO_2 content over Moscow (Ivanov, et al., 2012). According to satellite data the NO_2 tropospheric content over megacities reach high level (Hiboll et al., 2013). Our aerosol comparisons in urban and background conditions (Chubarova et al., 2011) also demonstrated the existence of the residual NO_2 contamination over Moscow, which can be seen in a specific character of AOT spectral difference between the parallel measurements in Moscow and in Zvenigorod background conditions at the distance of 55 km (see Fig.3 and the discussion in Chubarova et al., 2011). This residual NO_2 contamination is caused by much higher NO_2 content in Moscow than that accounted in the AERONET algorithm.

In order to exclude the effects of NO_2 underestimation in AOT retrievals over urban Moscow area we applied the algorithm for evaluating the NO_2 content, which has been developed recently (Chubarova et al., 2009, Chubarova et. al, 2010). For accounting the NO_2 amount up to the height of 350m we utilized the developed parameterizations of its content within 350m according to in-situ long-term NO_2 measurements in the boundary layer from ground to 350m in several points of Moscow (at the Ostankino tower and at the top of Moscow State University Building) during summer and winter conditions to account for possible differences in meteorological factors like boundary layer altitude, temperature and photochemistry effects. These data were combined with the results of photochemical model, which had been adapted to the available experimental data on different chemical constituents and meteorological conditions in the boundary layer. Input model parameters include spectral flux of solar radiation; absorption cross sections and quantum yields of photodissociation products; rate constants of chemical reactions; the altitude temperature profiles, turbulent diffusion coefficients, concentrations of some atmospheric components, and meteorological parameters which were measured during the experiments [Chubarova et al., 2010]. The applied 1-D photochemical model calculated the vertical profiles with 50-

meter resolution up to 20 km and takes into account for several hundreds of chemical reactions for 100 components. We also used the temperature profiles from Microwave Temperature Profiler MTP5 (Kadygrov et al., 2003) up to 600 m for the evaluation of the diffusion coefficients to account for the different boundary layer conditions. As a result, various weighting coefficients for summer and winter conditions were evaluated for different layers: 0-350m, 350-1000m, and 1000-2000 m. According to these data we obtained two regimes of NO_2 vertical distribution typical for Moscow conditions within the low 2 km layer. Note, that tropospheric and especially boundary layer NO_2 content in urban areas has the most important contribution to the total NO_2 content and is several times higher than that in background conditions (Richter et al., 2005, Hiboll et al., 2013). Therefore for the altitudes higher 2km we applied the climatological NO_2 values according to numerous data of aircraft measurements (Bruns et al. 2006, Heland et al., 2002, Martin et al., 2006). They are about 0.01 ppb for the altitudes of 2-5 km, and are characterized by linear decrease to approximately 0.01 ppb at 12 km. In the stratosphere the NO_2 profile corresponds to the data published in (Bruns, 2004) according to the direct measurements in Europe and Northern America. Totally the NO_2 content at the altitudes higher 2 km is relatively small comprising about 0.24 DU. ($0.6\ 10^{16}$ mol cm^{-2}).

Figure 5a and Table 1 show the resulting monthly mean NO_2 content obtained according to the proposed method. One can see that the maximum NO_2 content is observed in February and elevated NO_2 values are recorded in December-March period due to higher emissions from power stations during the heating season and larger NO_2 life time in winter conditions due to decreasing of the photodissociation rates at higher zenith angles (Brasseur and Solomon, 1986). Fig. 5a also demonstrates seasonal variations of NO_2 content, which is used in the standard AERONET algorithm. One can see that the new NO_2 climatology is 2-3 times higher than the standard AERONET NO_2 climatology, which is applied in the AERONET aerosol correction algorithm. Since these NO_2 amounts were obtained for the 2003-2005 period, we also compared them with the NO_2 retrievals over the same period according to the proposed method. As it is seen in Fig.5a, no any statistically significant difference between the revised NO_2 content climatology is detected between the 2002-2013 and 2003-2005 periods.

The values obtained from the new NO_2 climatology are well coincided with the results of accurate direct NO_2 retrievals using MAX-DOAS algorithm (Ivanov et al., 2012) over the same MSU MO site. We have a good agreement with these MAX-DOAS NO_2 estimates for 15 months of collocated observations. Mean difference between our NO_2 retrievals and the MAX-DOAS dataset is about -2±12% (at P=95%) for monthly mean NO_2 estimates, which were used for the NO_2 aerosol correction.

The estimated NO_2 optical thickness (OT_{NO2}) in different CIMEL spectral channels is shown in Fig.5b. The most pronounced effects of OT_{NO2}=0.02-0.03±0.003 are observed for 380 and 440nm channels due to the strongest NO_2 absorption there. At the same time, NO_2 optical thickness obtained

from the standard AERONET algorithm is much smaller and does not exceed OT_{NO2}=0.013 at 380nm in March. New NO_2 climatology provides NO_2 optical thickness, which is 2-4 times higher than the values in the standard AERONET dataset for Moscow urban conditions. It should be emphasized that the added OT_{NO2} values are close to the uncertainty threshold of aerosol optical thickness evaluation of ~0.02 at 340nm and are usually higher or comparable with the uncertainty threshold for AOT at other wavelengths especially, in winter and spring conditions, which should be necessary to take into account. The obtained monthly mean NO_2 content can be considered as a typical level for large megalopolis with 12 million residents and the NOx emission rates of about 100 $ktyr^{-1}$.

The effect of NO_2 content on the AOT retrievals is not very large and since there is no statistically significant trend in NO_2 content over Moscow according to our data as well as according to satellite retrievals (Hiboll et al., 2013, Shneider et al., 2015), we suggest to account only for monthly mean NO_2 values.

Since the uncertainty in AOT according to the additional correction on the revised NO_2 optical thickness has a spectral character the effect is also expressed in the retrievals of the Angstrom exponent (α). One can see in Table 1 a decrease (in absolute values) in the $\alpha_{440\text{-}870}$ retrievals of about 0.06-0.3 for different months mainly due to the reduction of AOT at 440nm after applying the higher values of OT_{NO2} from the new NO_2 climatology. On the contrary, the revised Angstrom exponent retrievals in UV spectral region increase up to 0.15-0.6 after additional NO_2 correction. Both procedures lead to decreasing in the second derivative of logarithm of AOT versus logarithm of wavelength (Eck et al., 1999) and may affect the inverse RT solution in the AERONET algorithm (Dubovik, King, 2000), especially in case, when OT_{NO2} values are close to aerosol optical thickness.

Seasonal variations of OT_{NO2} to AOT ratios at different wavelengths are shown in Figure 5c. One can see that the maximum effect is observed for the ratio at 380nm and 440nm, comprising about 15-20% in winter and 5-6% in other seasons. This ratio is smaller at 340 and 500 nm varying from 10% in winter to 2-3% in other seasons. The most substantial changes in aerosol properties and, hence, in solar irradiance due to NO_2 correction are observed during cold period. This implies the increase in the effects of NO_2 absorption during winter time.

We estimated relative attenuation due to monthly mean NO_2 and aerosol optical thickness for erythemal and longwave UV 300-380nm irradiance at ground using the TUV model (Madronich, Flocke, 1998) with 8-stream DISORT solver and pseudo spherical corrections. According to our estimates similar effects of NO_2 and AOT of about 4-7% are observed during winter time, while in summer the effects of AOT reach 14% compared with 1-2% due to NO_2 (Fig.5d). There is a pronounced amplification of NO_2 effects for longwave UV 300-380nm irradiance due to the increase of the effective wavelength (from ~305-315 nm for erythemal radiation to ~345nm – for UV irradiance 300-380nm), where the NO_2

absorption coefficients are much higher. In addition, using the on-line calculator (http://litms.molnet.ru/csif/index.php) developed in the Institute of Moleculer Physics of RRC "Kurchatov Institute" we estimated the effects of NO_2 on total shortwave irradiance, which are about 0.5% in summer and 2.5% in winter depending on NO_2 content and solar zenith angle.

As a result, we have applied the NO_2 correction to monthly mean AOT values for the whole AERONET dataset in Moscow since 2001. We should note, that large NO_2 content can be also observed in forest fire smoke plumes, however, due to large aerosol amount and small OT_{NO2}/AOT ratios its radiative effect should be small compared with the aerosol radiative impact.

Large NO_2 content has also the influence on the retrievals of other aerosol characteristics, which are not considered in this study. However, according to the previous cases study analysis we showed the pronounced effects of NO_2 on the retrievals of single scattering albedo, which can increase up to 0.02 when the ratio OT_{NO2}/AOT at 440nm is about 10% (Chubarova and Dubovik, 2004). The influence of NO_2 on the retrievals of aerosol size distribution is also pronounced with the artificial bias towards smaller particles with overestimating the fine mode fraction of about dV/dlnr= 0.02 $\mu m^3/\mu m^2$ at r=0.05-0.065 μm and the decrease over 0.01-0.03 $\mu m^3/mm^2$ at 0.11-0.15 μm for typical air pollution conditions (Chubarova and Dubovik, 2004). In overall, the fine mode fraction due to accounting for NO_2 content changes on 1-5%. We should note that in (Chubarova and Dubovik, 2004) only few cases (n=14) were analyzed while in this study we considered the NO_2 effects on AOT climatology over the whole period of measurements. In addition, in (Chubarova and Dubovik, 2004) the evaluation of the NO_2 content was made using the model vertical profile according to the global 3-D GEOS-CHEM model (Martin et al., 2002), while in this paper we applied the NO_2 profile in the low troposphere using the parameterizations obtained according to the in-situ NO_2 measurements up to 350meters and photochemical model directly for Moscow conditions.

A full scheme of aerosol correction for Moscow MSU MO aerosol measurements is shown in Fig.6. The final aerosol product is attributed to so-called level 2.5 just to be in the mainstream of the AERONET standard level ranks. Currently, the correction has been fulfilled only for the aerosol parameters retrieved from direct solar measurements (aerosol optical thickness and Angstrom exponent).

The standard and the revised monthly mean spectral AOT dependences over the 2001-2014 period with the application of the cloud and NO_2 corrections are shown in Fig.7. The revised spectral dependencies for most months especially in cold period, when NO_2 to AOT ratio is high, are characterized by more smooth spectral character due to the influence of spectral NO_2 correction. This correction also induces slightly higher determination coefficient when obtaining Angstrom exponent within 440-870nm in logarithmic space coordinates. The total difference in annual mean AOT values due

to the additional account for cloud and NO_2 corrections is about 0.04 in UV, 0.02 in visible, and 0.01 in near-infrared spectral ranges.

3.2 Seasonal changes in aerosol optical thickness in Moscow according to the revised dataset

After the additional cloud and NO_2 correction we obtained a revised dataset of aerosol optical thickness, water vapor content and Angstrom exponent over the 2001-2014 period. Fig.8 shows the seasonal changes of monthly mean AOT500, AOT380, and Angstrom exponent $\alpha_{440\text{-}870}$ from the revised dataset, the dataset with only additional cloud correction, and from the standard AERONET level 2.0 dataset. The difference between the cloud-corrected and the revised aerosol optical thickness demonstrates the effect of NO_2 additional correction. The revised AOT seasonal cycle is characterized by a pronounced summer maximum reaching AOT500=0.3 in August, an additional maximum in April (AOT500=0.22), and minimum in December and January (AOT500=0.08). One can see that the application of the additional cloud correction removes a local AOT maximum in February, and lowered the December artificial high AOT values. The application of the new NO_2 climatology provides the decrease in AOT all over the year and does not significantly change the AOT seasonal cycle. The maximum effects of NO_2 can be seen in correction of AOT at 380nm due to the highest NO_2 absorption coefficients. The effects of additional NO_2 and cloud correction are comparable for AOT380 and AOT440, while for AOT at other wavelengths the additional cloud correction plays more vital role. The main statistics of revised AOT, water vapor content and Angstrom exponent are presented in Table 2. It should be noted, that we have very small AOT statistics in December due to high cyclonic activity with cloudy weather. Moreover, the application of the restriction on air mass m>5, which can be observed in December even at noon conditions in Moscow, provides further elimination of the level 2.0 data. So the obtained climatological values should be taken with caution. However, after the additional corrections even this small dataset demonstrates reasonable AOT values, which are in agreement with the statistics obtained for January (next winter month) conditions (see Table 2).

In Moscow Angstrom exponent has a pronounced maximum in summer months, which had been also documented for European conditions (Hsu et al., 2014, Chubarova, 2009). The revised $\alpha_{440\text{-}870}$ values are characterized by much more noticeable seasonal dependence with a substantial decrease in December.

Figure 9 presents three-dimensional distributions of monthly mean, 50% quantile, maximum and minimum AOT500 values over the 2001-2014 period. The AOT maximum in spring (and, especially, in April) is typical for almost all years and is a characteristic feature for the whole Eastern European plane. It can be explained by the circulation pattern from South-East of Russia and Kazakhstan with dust

advection from semi-deserts and steppes, as well as by the accumulation of the dust after snow melting, and the beginning of agricultural season with the prescribed fires. At the same time, relatively small precipitation prevents wet deposition of aerosol particles and contributes to their accumulation. In April, for example, the precipitation is only 41 mm, which is about 30% smaller than the annual monthly mean value (Chubarova et al., 2014). The local June minimum is observed due to the increase in precipitation, dominating the northern air advection from Scandinavian regions, more intensive uptake of aerosol by grass and leaves, and comparatively high water store in soil and vegetation, which can also prevent active mineral dust aerosol formation. According to monthly mean data summer AOT500 maximum is observed in August. However, AOT500 50% quantile has the maximum in July, when the high temperature provides favorable conditions for the second aerosol generation and accumulation of aerosol (see also Fig.8 and Table 2). The bias towards the fall in monthly mean AOT500 is observed due to the episodes with forest and peat bog fires with high aerosol loading in 2002 (July, August and September) and 2010 (July, August) (Chubarova et al., 2012).

In winter, there is a minimum in AOT due to wet deposition of aerosol during active cyclonic processes and the absence of favorable conditions for second aerosol generation. Note, that low AOT in December and February are observed only after NO_2 and cloud correction.

The described AOT seasonal changes occur almost every year, except 2006 (see Fig.9). AOT daily maxima are also observed every year in spring and in summer. During the intensive forest fires in Moscow regions in 2002 and 2010 the daily maximum AOT500 has reached 2.3 in July 2002 and 3.7 in August 2010. However, there are no any seasonal changes in daily minima - the AOT500 varies within 0.02-0.05 throughout the year. Even during the long-term forest fires episodes very low and extremely high AOT values are observed during the same month. This phenomenon takes place due to changes in wind direction and the advection of fresh air as well as due to the effective wet deposition of aerosol particles from the atmosphere which, for example, was observed in August 2010.

3.3 Long-term AOT trends in Moscow and their possible reasons

The continuous aerosol measurements since 2001 provide a useful tool for studying long-term variability of aerosol properties over 14 years. Table 3 summarizes the correlation coefficients and AOT relative temporal changes for different months, except January and December, when the statistics is too low due to prevailing cloudy conditions. One can see a decrease in monthly mean AOT500 with the rate of about ~1-5% per year for most months, except June and November. However, the statistically significant trends of mean and daily maxima AOT500 values at P=95% are observed only in April, May and September. After excluding the intensive fire periods in 2002 and 2010 the significance of AOT trend remains the same, but its values have changed, for example, from 10% to 3% per year in September. In

April and September statistically significant negative trends were also obtained for 50% quantile AOT500. So we can state that the most significant AOT decrease is observed in spring and fall periods, however, negative tendencies are observed almost throughout a year.

Relative changes in annual mean and 50% quantile values of aerosol optical thickness at different wavelengths in UV, visible and near-infrared spectral range are shown in Fig.10. Negative annual AOT trends are about -2.3% and -1.7% per year at 500 nm, -2.7% and -2.9% per year at 340nm, and -1.8% and -1.1% per year at 1020 nm respectively for the mean and 50% quantile values. For the annual mean AOT the negative trend is statistically significant at P=95% over the whole spectral range and is characterized by a 15-20% drop over the last four years, while for annual 50% quantile AOT values the significant trend is observed only at 340 nm and at 500 nm. There is no statistically significant trend in the annual 50% quantile AOT at 1020 nm that could mean preserving the same coarse mode particles content in typical conditions. This could be also confirmed by the decrease in monthly mean Angstrom exponent obtained within a spectral range of 440-870nm during summer period. We should emphasize that the trend obtained for annual mean AOT values is much more sensitive to the fire smoke episodes with extremely high aerosol loading (for example, forest fires in 2002 and 2010). Annual 50% quantile AOT values are not sensitive to such outbursts, therefore their interannual changes better describe the temporal changes of typical aerosol.

The negative AOT trends in 21 century are observed over many regions in Europe. For example, according to satellite dataset Yoon et al., (2014) has revealed a distinct AOT decrease over western Europe of about −40% from 2003 to 2008. The same negative trends over 1997 to 2010 in Europe was obtained in (Hsu et al., 2012) according to SeaWiFS measurements. In Putaud et al (2014) the negative trends in AOT and some other aerosol characteristics were also obtained in Northern Italy over the 2004–2010 period.

There can be several natural or anthropogenic reasons for these negative AOT trends. In order to study the effect of anthropogenic emissions we used the officially reported emission data from the Centre on Emission Inventories and Projections WebDab – EMEP database (http://www.ceip.at/status_reporting/2014_submissions/). Fig 11a presents temporal variations in emissions of different main aerosol precursors over the European part of Russia, which can affect the secondary aerosol generation in Moscow. One can see a statistically significant at P=95% decrease in SO_x emission of about 135 Gg yr^{-1} per year (or 135 Gg yr^{-2}), the negative trend in emission of Non-methane volatile organic compound (NMVOC) of about 54 Gg yr^{-2}. In addition, the CO emissions, which do not influence directly on the secondary aerosol generation but may characterize the intensity of pollution from the transportation sources, has also a pronounced negative trend of about 69 Gg yr^{-2}. This negative trend also confirms the complex character of the atmosphere cleanup. There is also a tendency of NO_x

decrease over European part of Russia, especially during the last years but it is not statistically significant. Some negative tendency is observed in emissions of the particulate matter with the diameter less 2.5 μm (PM2.5). The comparison of temporal variability of main aerosol precursors over the European part of Russia and in Moscow is shown in Fig.11b. There we also present the trend in annual 50% quantile AOT500, which is not sensitive to the extremely high aerosol loading during the Moscow 2002 and 2010 fire episodes. One can see the absence of local changes in SO_x in Moscow compared with a distinct negative trend in SO_x up to -6.5% a year over the European part of Russia, which can be observed due to changes in fuel from coal to gas. In Moscow this change of fuel has been made earlier, at the end of 1980s. Note also, that the high median AOT values in 2006 correspond well with the elevated emission of SO_x both in Moscow and at the whole European part of Russia as well as the elevated emission of NO_x in Moscow. The last years are characterized by a decrease in NO_x emission both in Moscow and at the European part of Russia possibly due to improving the quality of petrol standards. As a result, we assume that negative trend in AOT is observed likely due to the decrease in anthropogenic emissions of SO_x and NMVOC over European part of Russia, which play a significant role in the second aerosol generation, especially during warm period. Some important role can also play the decrease in NO_2 emission during the last years since 2010.

However, natural AOT variations should be also taken into account. For example, since the AOT spatial distribution is characterized by a significant decrease from south-east to the north in Europe (Chubarova, 2009) natural AOT interannual variability can be observed due to the year-to-year variability of different air mass advection. We tested this effect and its possible influence on interannual AOT variability for the months with statistically significant negative trends - April, May, and September. For this purpose we compared the results obtained over the whole period of observations and over the last 5 years since 2010, when low 50% quantile AOT500 values were observed (see Fig.10b).

For this purpose we used the Hybrid Single-Particle Lagrangian Integrated Trajectory (HYSPLIT) model (Draxler and Hess, 1998) to generate the 24-hour backward trajectories for the days with AOT measurements in April, May and September at the altitude H=500m for 12:00 UTC. Since Moscow is located close to the center of the European Plain and there is almost the same probability of air parcel arriving from different directions, we combined the results in the standard wind diagram and compared the change in the relative number of cases in different directions over the whole period of measurements (2002-2014) with that over the last years (2010-2014). We will consider that the significant difference in circulation pattern occurs, when the change in relative number of cases over a particular direction exceeds 5%. In addition, we calculated the mean daily AOT500 for the air masses coming from different directions. Fig.12 presents the obtained wind diagrams as well as the mean daily AOT500 diagrams over these two periods. One can see that in most cases there is no significant difference in wind diagrams between 2010-2014 and 2002-2014 periods for all three months. The exception was observed in May with

small prevailing of air mass advection from the East (+7%), accompanied by slightly lower AOT (difference in AOT500=-0.02), and in September with small prevalence of the air mass advection from the North (+6%) accompanied by slightly higher AOT values (difference in AOT500=+0.03). Lower AOT500 values during the last 2010-2014 period were observed almost at all the directions of air mass advection with the difference of about 0.02÷0.14 in April, 0.02÷0.10 in May and 0.03÷0.18 in September. The increase in AOT500 higher than 0.01 was only observed in conditions with South-West air mass advection in April (difference in AOT500=+0.09), which occurrence is small, and in September with North and East air mass advection when there was a slight difference in AOT500=+0.03. Hence, we can state that there were no significant changes in circulation pattern during the last years. Note, that the data from September, 2002, when the intensive forest fires were observed and AOT500 was unusually high, were not used in this analysis.

Wet aerosol deposition, regulated by precipitation, can also play an important role in year-to-year AOT variability. In addition, the enhancement of the dynamic stability of the atmosphere can be an effective factor leading to the stagnation of air and, hence, to the aerosol accumulation. As a parameter characterizing the atmospheric instability we used the convective available potential energy (CAPE) (Barry and Chorley, 1998). The CAPE data from the ERA-Interim re-analysis over Moscow (36-38^{0}E, 55-56^{0}N) were taken for the days, when the aerosol measurements were made. As a result, multiple regression analysis has been applied for studying the relationship of monthly mean AOT500 with temperature (as an indicator of air advection), precipitation, wind speed, wind direction and CAPE characteristics according to the Moscow dataset over the whole period of measurements. However, the analysis revealed the absence of any significant AOT correlation with any of the characteristics considered. This means that natural factors might not be responsible for the negative AOT trend in the Moscow area.

In addition, we compared the changes of meteorological parameters, AOT500, the annual emissions of main aerosol precursors and PM2.5, observed during the last 2010-2014 period with their values for the whole dataset 2002-2014. We have to analyze the existing 2002-2013 dataset for emissions and assume, that they do not vary within the year, since the monthly resolution data are not available. All data were normalized against their means. Fig.13 shows error bars interval at confidence level P=95% of relatively changes over 2002-2014 in monthly mean AOT500, air temperature, precipitation, CAPE, as well as NMVOC, NO_x, PM2.5, SO_x emissions and, for comparison, the mean relative changes of these characteristics over the 2010-2014 period for April, May and September. One can see that the mean negative changes in emissions during the last 2010-2013 period were significantly higher than those over the whole period while the relative changes in meteorological factors demonstrate different signs, except the precipitation, which slightly increases in all months. Their mean relative changes lie mainly within the

602 error bars interval at P=95%, except air temperature in May, and CAPE in September. However, for the
603 other months these parameters have even the opposite sign, which might means the random character of
604 their change.

605 Hence, we should state that the effect of the negative trend in emission likely have the main
606 influence on negative AOT500 trend, which was observed over Moscow. There are some slight changes
607 in meteorological regime and advection, but they seems to be not very important.
608

609 ## 4 Discussion

610 We propose the additional cloud screening correction and the adjustment for the revised NO_2
611 content in large megacity conditions for obtaining the highest quality dataset of aerosol properties. Small
612 but systematical AOT500 overestimation up to 0.03 in the standard AERONET dataset was received due
613 to the effects of uniform upper layer clouds. This overestimation is usually higher than the uncertainty of
614 AOT measurements. However, in some months the application of additional cloud filter resulted in the
615 AOT bias of more than 0.1.

616 There can be some another drivers of increasing the AOT due to clouds as was obtained in several
617 recent publications both from ground-based and satellite dataset due to aerosol humidification growth,
618 cloud processing, or new particle formation in clouds (Quass et al., 2010, Eck et al., 2014). As a result,
619 we may consider two competing phenomena – the effects of cloud contamination on aerosol retrievals
620 and the possible changes in aerosol properties in the vicinity of clouds. We should note that since it is not
621 possible to distinct these two processes without special field experiments as it was made in (Eck et al.,
622 2014), our revised aerosol climatology relates to the classical way of aerosol properties evaluation, when
623 these aerosol/cloud interaction processes are not accounted for. However, the existence of the additional
624 cloud contaminated cases with solar disk blocking conditions almost in all cases, except 0.5% in winter,
625 biased the aerosol climatology. Their removal provides the better quality dataset.

626 The relative AOT500 difference between the standard dataset and the dataset with the additional
627 cloud-screening has minimum in summer (5%) and maximum up to 20-30% for winter months when the
628 occurrence of upper cloudiness is high, and AOT values are low. The larger AOT difference in winter can
629 be also attributed to more cloud filtering (with strict filter of human observed cloud fraction ≥60%) and
630 therefore highly likely larger differences with the standard AERONET values.

631 The application of an additional cloud filter results in significantly decrease in day number up to 7-
632 20% during warm period, and 25-45% during the cold period because of higher occurrence of overcast
633 upper layer cloudiness and the application of more strict filter NA<6. We should also note that the
634 susceptibility percentage of contaminated cases is in the qualitative agreement with the data shown in

635 Chew et al., (2011) as well as with the results obtained in (Huang et al. 2012) for the collocated
636 AERONET/CALIPSO and AERONET/MODIS measurements.

637 Since the effects of the proposed additional cloud-screening are distinct, its application may help in
638 obtaining the better quality aerosol datasets by different users, especially for the old, historical records.
639 However, we admit that this is not a rigorous assessment. But this additional correction could be very
640 useful in different applications. It is also possible to verify the current aerosol datasets using the cloud
641 data from the automatic total sky imagers, which have been already in operation at several sites (O'Neill
642 et al., 2003, Jeong, Li, 2010) or using the collocated lidar measurements (Chew et al, 2011, Huang et al.,
643 2012).

644 For additional NO_2 correction a new NO_2 content climatology over Moscow has been applied
645 according to the algorithm, which has been developed recently (Chubarova et. al, 2010) on the base of in-
646 situ NO_2 concentration measurements at different altitudes and the results of photochemical model. The
647 new monthly mean NO_2 content is two-three times higher, than that in the AERONET dataset, which is
648 used for aerosol correction due to extremely large NO_x emission in large megacity, like Moscow. The
649 most pronounced effects of OT_{NO2}=0.02-0.03 are observed at 380 and 440nm channels due to the
650 strongest NO_2 absorption. The obtained monthly mean NO_2 climatology can be considered as a typical
651 one for megalopolis conditions with 12 million residents and the NO_x emission rates of about 100 $ktyr^{-1}$
652 (Ivanov et al., 2012). The NO_2 correction over other megacities can be also made according to long-term
653 satellite NO_2 retrievals but after their rigorous validation. It should be emphasized that the upcoming
654 AERONET Version 3 database utilizes a new monthly mean climatology of total columnar NO_2 from the
655 OMI satellite sensor data and that these values are significantly higher than those obtained from the
656 SCIAMACHY database for the Moscow MSU MO site (T. Eck, personal communication).

657 Seasonal changes of OT_{NO2} to AOT ratio at 380 and 440nm vary from 15-20% in winter to 5-6%
658 in warm period. This ratio is much smaller at 340 and 500 nm changing from 10% in winter to 2-3% in
659 warm period. Hence, the most substantial changes in aerosol properties and, hence, in solar irradiance due
660 to NO_2 correction would be observed during cold period. According to radiative modeling this results in
661 similar effects of NO_2 and aerosol of about 4-7% in winter in the UV spectral region. For shortwave
662 irradiance the NO_2 effect in Moscow changes within 0.5-2.5% and also increases in winter.

663 The total difference in annual mean AOT values due to the additional account for cloud and NO_2
664 corrections is about 0.04 in UV, 0.02 in visible, and 0.01 in near-infrared spectral range. Note, that the
665 NO_2 correction mainly concerns the 340, 380, 440, and 500nm AOT channels and the retrievals of
666 Angstrom exponent. The revised aerosol product after the application of additional cloud and NO_2
667 correction is attributed to so-called level 2.5 to be in the mainstream of the AERONET standard level

ranks. Currently, the correction has been fulfilled only for the aerosol parameters retrieved from direct solar measurements (aerosol optical thickness, Angstrom exponent, and water vapor content).

The revised dataset of monthly mean aerosol optical thickness and Angstrom exponent in Moscow was used for studying seasonal changes as well as AOT long-term variability over the 2001-2014 period.

The corrected AOT mean seasonal cycle is characterized by a pronounced summer maximum, an additional spring maximum, and minimum in winter conditions (December-January). The application of the additional cloud correction removes a local AOT maximum in February, and lowered the December artificial high AOT values. Although we have only 4-day sample for December the application of additional correction provided reasonable changes removing the cloud contaminated cases with high optical thickness. However, still due to small statistics, the results for this month should be taken with caution. After the application of additional filters we also obtained much more noticeable seasonal dependence of Angstrom exponent with the maximum during summer period.

There are pronounced statistically significant negative trends at P=95% in temporal variation of mean and 50% quantile AOT500 values for some months over 2001-2014. We also found a decrease in monthly mean AOT500 changes of about -1-5% per year for most months, however, the statistically significant trends of mean and daily maxima AOT500 values are observed in April, May and September. The most significant temporal changes in AOT are observed in spring and fall period. This is especially important, since April is characterized by local seasonal AOT maximum. Removal of AOT observed during the intensive fire periods in 2002 and 2010 does not change the significance of the results, but modify the value of AOT500 relative change.

There is also a statistically significant negative trend at P=95% in annual mean AOT variations over the whole spectral range with a pronounced 15-20% drop during the last years. At the same time considering annual 50% quantile AOT variation we found a statistically significant trend in AOT only at 340 and 500 nm. No similar tendency in AOT at 1020 nm was obtained, that could mean no temporal changes in coarse mode particles during the whole period of observations in typical conditions, which are better described by the analysis of 50% quantile AOT.

To understand the cause of the negative trends we used the officially reported emission data from WebDab – EMEP database (http://www.ceip.at/status_reporting/2014_submissions/). According to these data we showed that the decrease in AOT in 21 century can be observed due to statistically significant at P=95% negative trends in SO_x emission of about 135 Gg yr^{-2}, in NMVOC emission of about 54 Gg yr^{-2}, which can affect the secondary aerosol generation. We found that the high median AOT values in 2006 correspond well with the elevated emission of SO_x both in Moscow and at the European part of Russia, as well as with NO_x – in Moscow. The last years are characterized by the decrease in NO_x emission both in

Moscow and at the European part of Russia possibly due to improving the quality of petrol standard. However, the NO_2 trend in Moscow and over European part of Russia is not statistically significant.

We also studied the possible effect of natural factors in interannual AOT variability. According to the 24-hour NOAA HYSPLIT model backward trajectory analysis at 500m AGL for 12h UTC we obtained the wind diagrams and the distribution of daily AOT500 at different directions of the air mass advection for the months with statistically significant negative AOT trends (April, May, September). However, no significant difference in wind diagram is observed over 2010-2014 compared with the 2002-2014 period for all three months except the small increase (+7%) in conditions with the East air mass advection, accompanied by slightly smaller AOT in May, and the small increase (+6%) of air mass advection from the North with slightly higher AOT values in September. At the same time we see a significant drop in AOT500 values almost at all directions, except South-West air mass advection in April, which occurrence is small, and in conditions with North and East air advection in September.

No statistically significant correlation was obtained in monthly mean AOT relationship with different meteorological parameters and CAPE. The analysis of relative changes in different characteristics obtained during the last years against the whole period of observations has revealed that mean negative changes in emissions of aerosol precursors over the 2010-2013 period were significantly higher than those over the whole period, while the relative changes in meteorological factors demonstrate different signs, except the precipitation, which slightly increased in all months. However, its changes are not statistically significant. This means the importance of the anthropogenic factor (negative emissions of aerosol precursors) for attributing the negative AOT trend in Moscow.

5 Conclusions

We show the necessity of additional cloud and NO_2 correction for retrieving the best quality aerosol climatology. The application of the additional cloud-screening filters revealed a noticeable positive bias of up to 0.03 in monthly mean aerosol optical thickness compared with the results obtained from the standard algorithm.

A new NO_2 climatology over Moscow has been obtained. Its application demonstrates that tropospheric NO_2 content in Moscow is two-three times larger than that applied in the standard AERONET algorithm. The additional NO_2 correction of aerosol optical thickness is about 0.01 at 340nm, and 0.015 – at 380 and 440nm.

The total difference in annual mean AOT values due to the additional account for cloud and NO_2 correction is about 0.04 in UV, 0.02 in visible, and 0.01 in near-infrared spectral range, which are higher

than the uncertainty of AOT measurements. The NO_2 correction mainly concerns the 340, 380, 440, and 500nm AOT channels and the retrievals of Angstrom exponent.

The revised dataset was used for the analysis of seasonal and year-to-year variability of aerosol optical thickness in Moscow over the 2001-2014 period. We have revealed the distinct seasonal cycle in AOT500 values changing from 0.08 in December up to 0.3 in August as well as summer maximum in Angstrom exponent.

The interannual changes in aerosol properties reveal distinct negative trends, which are statistically significant in April, May and September. We show that the main reason for the AOT decrease could be negative trends in emissions of different aerosol precursors over European Plain according to the WebDab – EMEP database. We showed that the AOT negative trend can be observed due to a noticeable decrease in SO_x, NMVOC emissions at the European Plain as well as due to the additional decrease in NO_x during the last years. The analysis of variability in natural factors has not revealed their significant influence on negative AOT trends. However, further studies will be helpful for understanding the role of specific emissions and their interaction with changing weather conditions.

Acknowledgements

We would like to thank the anonymous reviewer and Dr. Thomas Eck for very helpful comments and Dr. Alexander Smirnov (NASA Goddard Space Flight Center) for fruitful discussions. The authors gratefully acknowledge the NOAA Air Resources Laboratory (ARL) for the provision of the HYSPLIT transport and dispersion model and/or READY website (http://www.ready.noaa.gov) used in this publication. The work was partially supported by RFBR grants #13-05-00956 and #15-05-03612.

References

Barry, R.G. and Chorley, R.J.: Atmosphere, weather and climate (7th ed.) Routledge, p. 80-81, 1998.

Brasseur, G., Solomon S., Aeronomy of the Middle Atmosphere. Springer, Netherlands, 452 p., 1986.

Bruns, M.: NO2 retrieval using Airborne Multi Axis Differential Optical Absorption Spectrometer (AMAXDOAS) data, Dissertation, Universitat Bremen, 174 p. 2004.

Bruns, M., Buehler, S. A., Burrows, J. P., Richter, A., Rozanov, A., Wang, P., Heue, K. P., Platt, U., Pundt, I., and Wagner, T.: NO2 Profile retrieval using airborne multi axis UV-visible skylight absorption measurements over central Europe, Atmos. Chem. Phys., 6, 3049-3058, doi:10.5194/acp-6-3049-2006, 2006.

764 Chew B. N., Campbell J. R., Reid J. S., Giles D. M., Welton E. J., Salinas S.V., Liew S.C. Tropical cirrus
765 cloud contamination in sun photometer data, Atmospheric Environment, 45, (2011) 6724e6731, 2011.

766 Chubarova, N. Y.: Seasonal distribution of aerosol properties over Europe and their impact on UV
767 irradiance, Atmos. Meas. Tech., 2, 593-608, doi:10.5194/amt-2-593-2009, 2009.

768 Chubarova, N. and Dubovik, O.: The sensitivity of aerosol properties retrievals from AERONET
769 measurements to NO_2 concentration over industrial region on the example of Moscow. Optica Pura y
770 Aplicada, A. Hidalgo (Spain), 37, № 3, p. 3315-3319, 2004.

771 Chubarova, N.Ye, Larin, I.K., Lebedev, V.V., Partola, V., Lezina, E.A., and Rublev A.N.: Experimental
772 and Model Study of Changes in Spectral Solar Irradiance in the Atmosphere of Large City due to
773 Tropospheric NO_2 Content. Current Problems in Atmospheric Radiation. Proceedings of the International
774 Radiation Symposium (IRC/IAMAS), AIP Conference Proceedings 1100, p. 459-462,
775 10.1063/1.3117019, 2009.

776 Chubarova, N.E., Larin, I.K., Lezina, E.A.: Experimental studies and modeling of nitrogen dioxide
777 variations in the lowest troposphere layer in Moscow , Newsletter Moscow State University, series 5,
778 Geography, 5, № 2, p. 11-18, 2010.

779 Chubarova, N., Nezval', Ye., Sviridenkov, I., Smirnov, A., and Slutsker, I.: Smoke aerosol and its
780 radiative effects during extreme fire event over Central Russia in summer 2010, Atmos. Meas. Tech., 5,
781 557-568, doi:10.5194/amt-5-557-2012, 2012.

782 Chubarova, N.E., Nezval', E.I., Belikov, I.B., Gorbarenko, E.V., Eremina, I.D., Zhdanova, E.Yu,
783 Korneva, I.A., Konstantinov, P.I., Lokoshchenko, M.A., Skorokhod, A.I., and Shilovtseva O.A.: Climatic
784 and environmental characteristics of Moscow megalopolis according to the data of the Moscow State
785 University Meteorological Observatory over 60 years Russian Meteorology and Hydrology, Allerton
786 Press Inc. (United States), 39, № 9, p. 602-613, 2014.

787 Chubarova, N.Y., Sviridenkov, M.A., Smirnov, A., and Holben, B.N.: Assessments of urban aerosol
788 pollution in Moscow and its radiative effects, Atmos. Meas. Tech., N 4, pp. 367-378, 2011.

789 Coen, C., Andrews, M.E., Asmi, A., Baltensperger, U., Bukowiecki, N., Day, D., Fiebig, M., Fjaeraa, A.
790 M., Flentje, H., Hyvärinen, A., Jefferson, A., Jennings, S. G., Kouvarakis, G., Lihavainen, H., Lund
791 Myhre, C., Malm, W. C., Mihapopoulos, N., Molenar, J. V., O'Dowd, C., Ogren, J. A., Schichtel, B. A.,
792 Sheridan, P., Virkkula, A., Weingartner, E., Weller, R., and Laj, P.: Aerosol decadal trends – Part 1: In-
793 situ optical measurements at GAW and IMPROVE stations, Atmos. Chem. Phys., 13, 869-894,
794 doi:10.5194/acp-13-869-2013, 2013.

795 Draxler, R.R., and G.D. Hess, 1998: An overview of the HYSPLIT_4 modeling system of trajectories,
796 dispersion, and deposition. Aust. Meteor. Mag., 47, 295-308.

797 Dubovik, O. and King, M. D.: A flexible inversion algorithm for retrieval of aerosol optical properties
798 from Sun and sky radiance measurements, J. Geophys. Res., 105(D16), 20673–20696, 2000.

799 Eck, T. F., Holben, B. N., Reid, J. S., Dubovik, O., Smirnov, A., O'Neill, N. T., Slutsker, I., and Kinne,
800 S.: Wavelength dependence of the optical depth of biomass burning, urban and desert dust aerosols, J.
801 Geophys. Res., 104(D24), 31333–31349, 1999.

802 Eck, T. F., Holben, B. N., Reid, J. S., Giles, D. M., Rivas, M.A., Singh, R. P., Tripathi, S. N., Bruegge, C.
803 J., Platnick, S.,Arnold, G. T., Krotkov, N. A., Carn, S. A., Sinyuk, A., Dubovik, O., Arola, A., Schafer, J.
804 S., Artaxo, P., Smirnov, A., Chen, H.,and Goloub, P.: Fog- and cloud-induced aerosol modification
805 observed by the Aerosol Robotic Network (AERONET), J. Geophys.Res., 117, D07206,
806 doi:10.1029/2011JD016839, 2012.

807 Eck, T. F., Holben, B. N., Reid, J. S., Arola, A., Ferrare, R. A., Hostetler, C. A., Crumeyrolle, S. N.,
808 Berkoff, T. A., Welton, E. J., Lolli, S., Lyapustin, A., Wang, Y., Schafer, J. S., Giles, D. M., Anderson, B.
809 E., Thornhill, K. L., Minnis, P., Pickering, K. E., Loughner, C. P., Smirnov, A., and Sinyuk, A.:
810 Observations of rapid aerosol optical depth enhancements in the vicinity of polluted cumulus clouds,
811 Atmos. Chem. Phys., 14, 11633-11656, doi:10.5194/acp-14-11633-2014, 2014.

812 Elansky, N. F., Lokoshchenko, M. A., Belikov, I. B., Skorokhod, A. I., and Shumskii, R. A.: Variability
813 of trace gases in the atmospheric surface layer from observations in the city of Moscow, Izvestiya,
814 Atmospheric and Oceanic Physics, V. 43, 2 , pp. 219-231, 2007.

815 Eskes, H.J. and Boersma, K.F.: Averaging kernels for DOAS total-column satellite retrievals, Atmos.
816 Chem. Phys.3, 1285-1291, 2004.

817 Evnevich, T. V., and I. A. Savikovskij, Calculation of direct solar radiation and coefficient of atmospheric
818 transparency (in Russian), Meteorol. Gydrol., 5, 106– 109. 1989.

819 Handbook of Clouds and Cloudy Atmosphere (Eds. I. P. Mazin and A.H. Hrgian), Hydromet Publishing
820 House, Leningrad, 647 pp, 1989.

821 Heland, J., Schlager, H., Richter, A.. and J.P. Burrows: First comparison of tropospheric NO_2 column
822 densities retrieved from GOME measurements and in situ aircraft profile measurements. Geophysical
823 Research Letters, VOL. 29, NO.20,1983, 2002.

824 Hilboll, A., Richter, A., and Burrows, J. P.: Long-term changes of tropospheric NO2 over megacities
825 derived from multiple satellite instruments, Atmos. Chem. Phys., 13, 4145-4169, doi:10.5194/acp-13-
826 4145-2013, 2013.

827 Holben, B. N., Eck, T. F., Slutsker, I., Tanre, D., Buis, J. P., Setzer, A., Vermote, E., Reagan, J. A.,
828 Kaufman, Y. J., Nakajima, T., Lavenu, F., Jankowiak, I., and Smirnov, A.: AERONET – A federated
829 instrument network and data archive for aerosol characterization, Remote Sens. Environ., 66, 1–16, 1998.

830 Holben, B.N., D.Tanre, A.Smirnov, T.F.Eck, I.Slutsker, N.Abuhassan, W.W.Newcomb, J.Schafer,
831 B.Chatenet, F.Lavenue, Y.J.Kaufman, J.Vande Castle, A.Setzer, B.Markham, D.Clark, R.Frouin,
832 R.Halthore, A.Karnieli, N.T.O'Neill, C.Pietras, R.T.Pinker, K.Voss, and G.Zibordi, 2001: An emerging
833 ground-based aerosol climatology: Aerosol Optical Depth from AERONET, J. Geophys. Res., 106, 12
834 067-12 097.

835 Holben, B. N., Eck, T., Slutsker, I., Smirnov, A., Sinyuk, A., Schafer, J., Giles, D., and Dubovik, O.:
836 AERONET Version 2.0 quality assurance criteria, in: Remote Sensing of the Atmosphere and Clouds,
837 edited by: Tsay, S.-C., Nakajima, T., Singh, R. P., and Sridharan, R., Proc. of SPIE, Goa, India, 13–17
838 November, 6408, 2006.

839 Hsu, N. C., Gautam, R., Sayer, A. M., Bettenhausen, C., Li, C., Jeong, M. J., Tsay, S.-C., and Holben, B.
840 N.: Global and regional trends of aerosol optical depth over land and ocean using SeaWiFS measurements
841 from 1997 to 2010, Atmos. Chem. Phys., 12, 8037-8053, doi:10.5194/acp-12-8037-2012, 2012.

842 Huang, J., Hsu C., Tsay S.-C., Holben B. N., Welton E. J., Smirnov A., Jeong M. J., Hansell R. A.,
843 Berkoff T.A., Liu Z., Liu G.-R., Campbell J. R., Liew S. C., and Barnes J. E. Evaluations of cirrus
844 contamination and screening in ground aerosol observations using collocated lidar systems, J. Geophys.
845 Res., 117, D15204, doi:10.1029/2012JD017757. 2012

846 International Cloud Atlas, Volume 11, WMO, 1987, ISBN 92 - 63 - L2407 – 8.

847 IPCC, 2013: Climate Change 2013: The Physical Science Basis. Contribution of Working Group I to the
848 Fifth Assessment Report of the Intergovernmental Panel on Climate Change. Cambridge University
849 Press, Cambridge, United Kingdom and New York, NY, USA, 1535 pp. 2013.

850 Ivanov V. A., Elokhov A. S., and Postylyakov O. V.: On the Possibility of Estimating the Volume of
851 NO2 Emissions in Cities Using Zenith Spectral Observations of Diffuse Solar Radiation near 450 nm.
852 Atmospheric and Oceanic Optics, 2012, Vol. 25, No. 6, pp. 434–439. 2012.

853 Jeong M.J., Li, Z.: Separating real and apparent effects of cloud, humidity, and dynamics on aerosol
854 optical thickness near cloud edges, V.115, D00K32, DOI: 10.1029/2009JD013547, 2010.

855 Kadygrov E.N., Shur G. N., and Viazankin A. S.: Investigation of atmospheric boundary layer
856 temperature, turbulence, and wind parameters on the basis of passive microwave remote sensing. Radio
857 Science, V. 38, No. 3, 8048, doi:10.1029/2002RS002647, 2003.

858 Kanaya, Y., Irie, H., Takashima, H., Iwabuchi, H., Akimoto, H., Sudo, K., Gu, M., Chong, J., Kim, Y. J.,
859 Lee, H., Li, A., Si, F., Xu, J., Xie, P.-H., Liu, W.-Q., Dzhola, A., Postylyakov, O., Ivanov, V., Grechko,
860 E., Terpugova, S., and Panchenko, M.: Long-term MAX-DOAS network observations of NO2 in Russia
861 and Asia (MADRAS) during the period 2007–2012: instrumentation, elucidation of climatology, and
862 comparisons with OMI satellite observations and global model simulations, Atmos. Chem. Phys., 14,
863 7909-7927, doi:10.5194/acp-14-7909-2014, 2014.

864 Loeb, N. G., and G. L. Schuster, An observational study of the relationship between cloud, aerosol and
865 meteorology in broken low-level cloud conditions, J. Geophys. Res., 113, D14214,
866 doi:10.1029/2007JD009763, 2008.

867 Martin, RV, Chance, K., Jacob, D.J., Kurosu, T.P., Spurr, R.J.D., Bucsela, E., Gleason, J.F., Palmer, P.I,
868 Bey, I., Fiore, A.M., Li, Q., Yantosca, R.M., and Koelemeijer, R.B.A.: An improved retrieval of
869 tropospheric nitrogen dioxide from GOME, Journal of Geophysical Research, V. 107, No. D20, ACH 9,
870 pp. 1-21., 10.1029/2001JD001027, 2002.

871 Martin, R.V., Sioris, C.E., Chance, K., Ryerson, Th. B., Wooldridge, P. J., Cohen, R. C., Neuman, J. A.,
872 Swanson, A., and Flocke, F. M.: Evaluation of space-based constraints on global nitrogen oxide
873 emissions with regional aircraft measurements over and downwind if eastern North America, Journal of
874 Geophysical Research,vol.111, 2006.

875 Madronich S., Flocke S., in: P. Boule (Ed.), Handbook of Environmental Chemistry, Springer-Verlag,
876 Heidelberg, p. 1–26.1998.

877 Ohvril, H., Teral H., Neiman L., Uustare M., Tee M., Russak V., Kallis A., Okulov O., Terez E., Terez
878 G., Guschin G., Abakumova G., Gorbarenko E., Tsvetkov A., and Laulainen N. Global dimming and
879 brightening versus atmospheric column transparency, Europe, 1906–2007, J. Geophys. Res., 114,
880 D00D12, doi:10.1029/2008JD010644, 2009.

881 O'Neill, N.T., Eck, T.F., Holben, B.N., Smirnov, A., and Dubovik, O.: Bimodal size distribution
882 influences on the variation of Angstrom derivatives in spectral and optical depth space … - Journal of
883 Geophysical Research: Atmospheres, 2001.

884 O'Neill, N. Eck, T. F., Smirnov, A., Holben, B. N., and Thulasiraman, S.: Spectral discrimination of
885 coarse and fine mode optical depth, Vol.. 108, J. Geophys. Res., No. D17, 4559-4573,
886 10.1029/2002JD002975, 2003.

887 Putaud, J. P., Cavalli, F., Martins dos Santos, S., and Dell'Acqua,A.: Long-term trends in aerosol optical
888 characteristics in the Po Valley, Italy, Atmos. Chem. Phys., 14, 9129-9136, doi:10.5194/acp-14-9129-
889 2014, 2014.

Report on the State of the Environment in Moscow in 2013. The Department for nature use and environment protection of Moscow Government. Eds. Kulbachevski, (In Russian). http://www.mosecom.ru/reports/2013/report2013.pdf, 224p., 2014.

Richter, A., Burrows, J. P., Nüß, H., Granier, C., Niemeier, U. Increase in tropospheric nitrogen dioxide over China observed from space. Nature, 437, 129-132, 2005.

Uliumdzhieva, N., Chubarova, N., and Smirnov, A.: Aerosol characteristics of the atmosphere over Moscow from Cimel sun photometer data, Meteorol. Hydrol., 1, 48–57, 2005.

Schneider P., W. A. Lahoz, and R. van der A., Recent satellite-based trends of tropospheric nitrogen dioxide over large urban agglomerations worldwide. Atmos.Chem. Phys., 15, 1205–1220, 2015.

Smirnov, A., Holben, B., Eck, T., Dubovik, O., and Slutsker, I.: Cloud screening and quality control algorithms for the AERONET data base, Remote Sens. Environ., 73, 337–349, 2000.

Su, W., G. L. Schuster, N. G. Loeb, R. R. Rogers, R. A. Ferrare, C. A. Hostetler, J. W. Hair, and M. D. Obland, Aerosol and cloud interaction observed from high spectral resolution lidar data, J. Geophys. Res., 113, D24202, doi:10.1029/2008JD010588, 2008.

Tegen, I., Hollrig, P., Chin, M., Fung, I., Jacob, D., Penner, J.: Contribution of different aerosol species to the global aerosol extinction optical thickness: Estimates from model results, J. Geophys. Res., 102(D20), 23895–23915, doi:10.1029/97JD01864, 1997.

Yoon, J., Burrows, J. P., Vountas, M., von Hoyningen-Huene, W., Chang, D. Y., Richter, A., and Hilboll, A.: Changes in atmospheric aerosol loading retrieved from space-based measurements during the past decade, Atmos. Chem. Phys., 14, 6881-6902, doi:10.5194/acp-14-6881-2014, 2014.

WMO, Revised Instruction Manual on Radiation Instruments and Measurements. WCRP Publications Series, No 7, WMO/TD, No.149, 1986.

915 List of the Tables:

916 Table 1. The monthly mean total NO_2 content according to the new climatology and NO_2 used in
917 the standard AERONET algorithm; total NO_2 optical thickness at different wavelengths, and the
918 difference in Angstrom exponent obtained with and without additional NO_2 correction of aerosol optical
919 thickness at different wavelengths. Moscow, 2002-2013.

920

months	total* NO_2 content, DU*	NO_2 content used in the standard AERONET algorithm	total* NO_2 optical thickness at different wavelengths, nm				difference in Angstrom exponent	
			340	380	440	500	440-870nm	340-380nm
1	1.69	0.401	0.018	0.027	0.023	0.010	-0.22	0.55
2	1.96	0.607	0.022	0.032	0.027	0.012	-0.15	0.38
3	1.82	0.809	0.020	0.029	0.025	0.011	-0.10	0.24
4	1.60	0.429	0.017	0.026	0.022	0.010	-0.08	0.21
5	1.35	0.373	0.015	0.022	0.018	0.008	-0.08	0.21
6	1.13	0.278	0.012	0.018	0.015	0.007	-0.09	0.22
7	1.29	0.526	0.014	0.021	0.018	0.008	-0.05	0.13
8	1.34	0.474	0.015	0.022	0.018	0.008	-0.05	0.12
9	1.23	0.297	0.013	0.020	0.017	0.007	-0.07	0.16
10	1.24	0.371	0.014	0.020	0.017	0.007	-0.11	0.29
11	1.47	0.518	0.016	0.024	0.020	0.009	-0.18	0.44
12	1.62	0.285	0.018	0.026	0.022	0.010	-0.33	0.78
year	1.48	0.45	0.02	0.02	0.02	0.01	-0.13	0.31

921 *- total NO_2 content partly includes the NO_2 content which is applied in the standard
922 AERONET correction algorithm.

923

924

925 Table 2. The main statistics of aerosol optical thickness at different wavelengths, water vapor content, and
926 Angstrom exponent $\alpha_{440\text{-}870}$ in Moscow. The revised AERONET dataset. 2001-2014.
927

Months	1	2	3	4	5	6	7	8	9	10	11	12	year average
Day number	33	68	144	191	227	244	290	243	186	87	33	4	146
mean													
AOT340	0.12	0.23	0.25	0.36	0.32	0.25	0.38	0.46	0.38	0.22	0.17	0.12	0.27
AOT380	0.11	0.20	0.22	0.31	0.28	0.22	0.33	0.41	0.34	0.19	0.15	0.11	0.24
AOT440	0.09	0.17	0.19	0.26	0.23	0.18	0.27	0.35	0.29	0.16	0.13	0.09	0.20
AOT500	0.08	0.14	0.16	0.22	0.19	0.15	0.23	0.30	0.25	0.14	0.11	0.08	0.17
AOT675	0.05	0.09	0.10	0.14	0.12	0.09	0.14	0.19	0.16	0.09	0.07	0.06	0.11
AOT870	0.04	0.07	0.08	0.10	0.09	0.07	0.09	0.13	0.11	0.06	0.05	0.04	0.08
AOT1020	0.04	0.07	0.07	0.08	0.08	0.06	0.07	0.10	0.09	0.05	0.05	0.05	0.07
H20 content, cm	0.27	0.29	0.50	0.70	1.35	1.69	2.21	2.02	1.55	0.91	0.58	0.37	1.04
Angstrom exponent	1.24	1.30	1.27	1.39	1.35	1.50	1.63	1.55	1.47	1.35	1.30	1.30	1.39
standard deviation													
AOT340	0.09	0.15	0.19	0.26	0.19	0.15	0.29	0.50	0.42	0.15	0.12	0.04	0.21
AOT380	0.08	0.14	0.17	0.23	0.17	0.13	0.26	0.48	0.39	0.14	0.11	0.04	0.20
AOT440	0.07	0.12	0.14	0.19	0.14	0.11	0.23	0.45	0.34	0.12	0.09	0.04	0.17
AOT500	0.06	0.10	0.12	0.15	0.11	0.09	0.19	0.41	0.30	0.10	0.07	0.04	0.14
AOT675	0.04	0.07	0.08	0.09	0.07	0.05	0.12	0.29	0.19	0.06	0.05	0.04	0.09
AOT870	0.02	0.05	0.05	0.06	0.05	0.04	0.07	0.20	0.13	0.04	0.03	0.03	0.06
AOT1020	0.02	0.04	0.04	0.04	0.05	0.03	0.05	0.15	0.09	0.03	0.03	0.02	0.05
H20 content, cm	0.12	0.09	0.25	0.28	0.56	0.54	0.50	0.53	0.47	0.41	0.28	0.14	0.35
Angstrom exponent	0.24	0.28	0.29	0.23	0.29	0.25	0.17	0.18	0.21	0.24	0.16	0.35	0.24
confidence interval P=95%													
AOT340	0.03	0.04	0.03	0.04	0.02	0.02	0.03	0.06	0.06	0.03	0.04	0.04	0.04
AOT380	0.03	0.03	0.03	0.03	0.02	0.02	0.03	0.06	0.06	0.03	0.04	0.04	0.03
AOT440	0.02	0.03	0.02	0.03	0.02	0.01	0.03	0.06	0.05	0.02	0.03	0.04	0.03
AOT500	0.02	0.02	0.02	0.02	0.01	0.01	0.02	0.05	0.04	0.02	0.02	0.04	0.03
AOT675	0.01	0.02	0.01	0.01	0.01	0.01	0.01	0.04	0.03	0.01	0.02	0.04	0.02
AOT870	0.01	0.01	0.01	0.01	0.01	0.00	0.01	0.02	0.02	0.01	0.01	0.03	0.01
AOT1020	0.01	0.01	0.01	0.01	0.01	0.00	0.01	0.02	0.01	0.01	0.01	0.02	0.01
H20 content, cm	0.04	0.02	0.04	0.04	0.07	0.07	0.06	0.07	0.07	0.09	0.10	0.14	0.07
Angstrom	0.08	0.07	0.05	0.03	0.04	0.03	0.02	0.02	0.03	0.05	0.05	0.34	0.07

exponent,													
						50%quantile							
AOT340	0.11	0.18	0.23	0.37	0.32	0.24	0.35	0.32	0.28	0.18	0.16	0.12	0.24
AOT380	0.10	0.15	0.21	0.32	0.27	0.21	0.30	0.29	0.25	0.15	0.14	0.10	0.21
AOT440	0.08	0.13	0.17	0.26	0.22	0.17	0.25	0.24	0.21	0.13	0.12	0.08	0.17
AOT500	0.07	0.11	0.14	0.22	0.19	0.15	0.21	0.20	0.18	0.12	0.11	0.07	0.15
AOT675	0.05	0.08	0.09	0.14	0.12	0.09	0.13	0.13	0.11	0.07	0.07	0.04	0.09
AOT870	0.04	0.06	0.07	0.10	0.09	0.07	0.09	0.08	0.08	0.05	0.05	0.03	0.07
AOT1020	0.04	0.06	0.06	0.08	0.07	0.06	0.07	0.07	0.06	0.04	0.05	0.04	0.06
H20 content, cm	0.28	0.29	0.48	0.70	1.45	1.69	2.17	2.11	1.57	0.87	0.52	0.41	1.04
Angstrom exponent	1.46	1.40	1.42	1.49	1.41	1.59	1.69	1.61	1.54	1.47	1.39	1.72	1.52
						maximum							
AOT340	0.37	0.62	1.10	1.52	1.37	0.87	3.19	3.79	2.90	0.77	0.70	0.20	1.45
AOT380	0.34	0.58	0.95	1.34	1.20	0.76	2.97	3.78	2.74	0.70	0.60	0.17	1.35
AOT440	0.30	0.51	0.79	1.10	0.96	0.66	2.60	3.63	2.46	0.57	0.48	0.16	1.18
AOT500	0.27	0.45	0.65	0.89	0.77	0.57	2.25	3.46	2.16	0.45	0.39	0.15	1.04
AOT675	0.18	0.32	0.42	0.51	0.42	0.36	1.42	2.66	1.41	0.27	0.26	0.12	0.70
AOT870	0.13	0.24	0.32	0.31	0.29	0.24	0.89	1.85	0.89	0.18	0.19	0.09	0.47
AOT1020	0.10	0.20	0.28	0.24	0.28	0.22	0.64	1.41	0.65	0.15	0.17	0.08	0.37
H20 content, cm	0.60	0.52	1.39	1.80	3.11	3.16	3.46	3.53	2.82	2.11	1.29	0.55	2.03
Angstrom exponent	1.86	1.89	1.86	1.93	1.98	2.12	2.11	1.94	1.96	1.88	1.72	1.82	1.92
						minimum							
AOT340	0.03	0.05	0.06	0.04	0.08	0.05	0.10	0.08	0.07	0.07	0.05	0.11	0.07
AOT380	0.03	0.04	0.03	0.03	0.06	0.03	0.05	0.04	0.04	0.04	0.02	0.07	0.04
AOT440	0.02	0.03	0.03	0.03	0.05	0.03	0.05	0.04	0.03	0.03	0.02	0.05	0.04
AOT500	0.02	0.02	0.03	0.03	0.04	0.03	0.05	0.04	0.03	0.03	0.02	0.05	0.03
AOT675	0.01	0.02	0.02	0.02	0.03	0.02	0.03	0.02	0.02	0.02	0.02	0.03	0.02
AOT870	0.01	0.02	0.02	0.02	0.03	0.02	0.02	0.02	0.02	0.02	0.01	0.02	0.02
AOT1020	0.02	0.03	0.02	0.02	0.02	0.01	0.01	0.01	0.01	0.02	0.02	0.02	0.02
H20 content, cm	0.07	0.11	0.16	0.20	0.50	0.64	1.12	0.90	0.53	0.24	0.21	0.16	0.40
Angstrom exponent	0.96	0.72	0.56	0.82	0.42	0.43	1.04	1.02	0.44	0.86	1.01	0.96	0.77

928

929

930

Table 3. Correlation coefficients and AOT500 trends (%yr^{-1}) over 2001-2014 in monthly mean, 50% quantile and daily maxima. Statistically significant values at P= 95% are shown in bold. Moscow.

months	average		50% quantile		daily maxima	
	correlation coefficient	trend,%yr^{-1}	correlation coefficient	trend,%yr^{-1}	correlation coefficient	trend,%yr^{-1}
2	-0.14	-2%	-0.08	-1%	-0.28	-4%
3	-0.30	-3%	-0.36	-4%	-0.09	-1%
4	**-0.67**	**-5%**	**-0.64**	**-7%**	**-0.48**	**-4%**
5	**-0.52**	**-2%**	0.19	1%	**-0.69**	**-6%**
6	-0.04	0%	0.00	0%	0.02	0%
7*	-0.38 /-0.51	-3%/-1%	-0.10/-0.14	-1%/-1%	-0.46/-0.18	-10%/-1%
8*	0.01/-0.47	0%/-1%	0.03/-0.19	1%/-1%	0.04/-0.14	1%/-1%
9*	**-0.50/-0.50**	**-10%-3%**	**-0.48**/-0.43	**-10%**/-3%	**-0.58/-0.72**	**-14%/-7%**
10	-0.05	-1%	-0.08	-1%	-0.04	-1%
11	0.09	1%	0.09	1%	0.05	1%

* - first value corresponds to the whole statistics and the second one - to the statistics without forest fires episodes observed in 2002 and 2010.

941

942

943

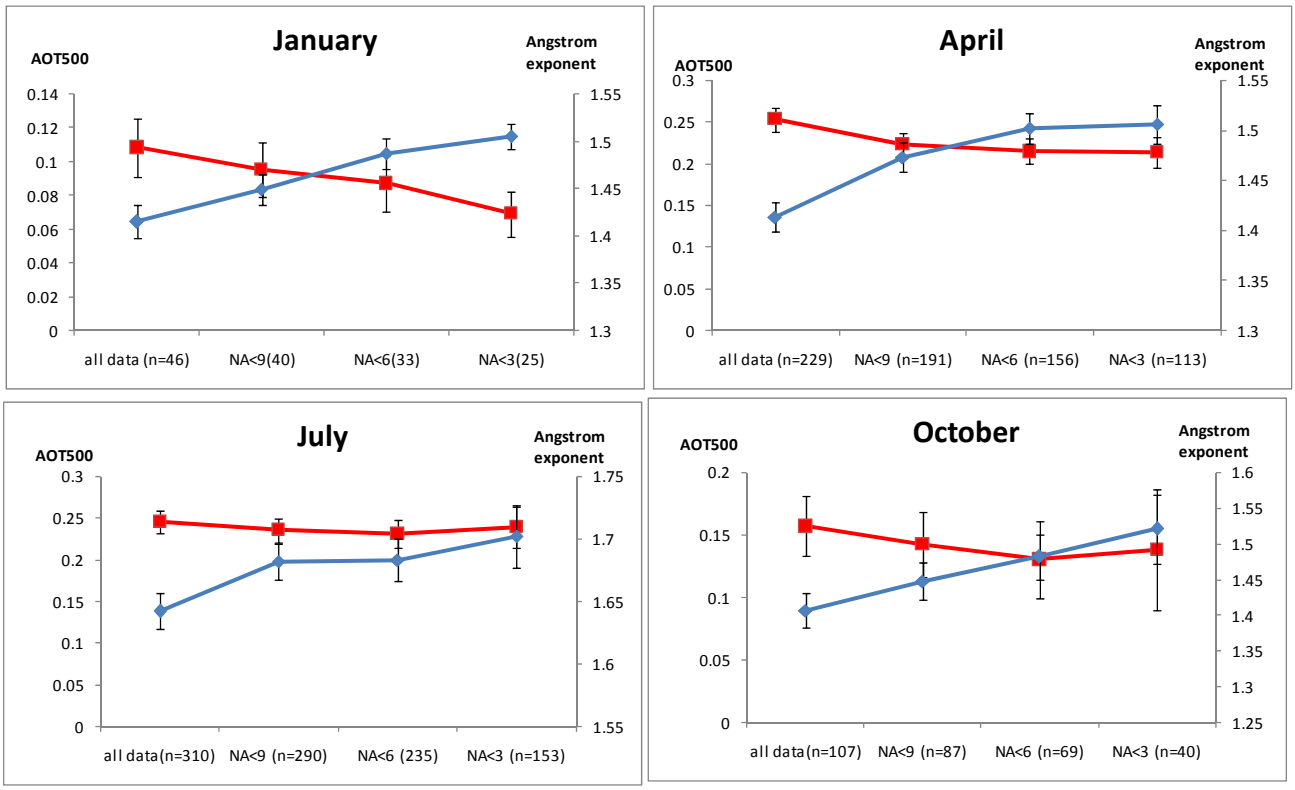

944

945 Fig.1. Mean aerosol optical thickness at 500nm (AOT500) and Angstrom exponent within 440-870 nm
946 spectral range in different samples with various total cloud amount (NA) thresholds for the central months
947 of the seasons. Moscow, 2001-2014. Number of days with measurements for each sample is given in
948 brackets. Note, that the error bars are shown at the confidence level P=80%.

949

950

951

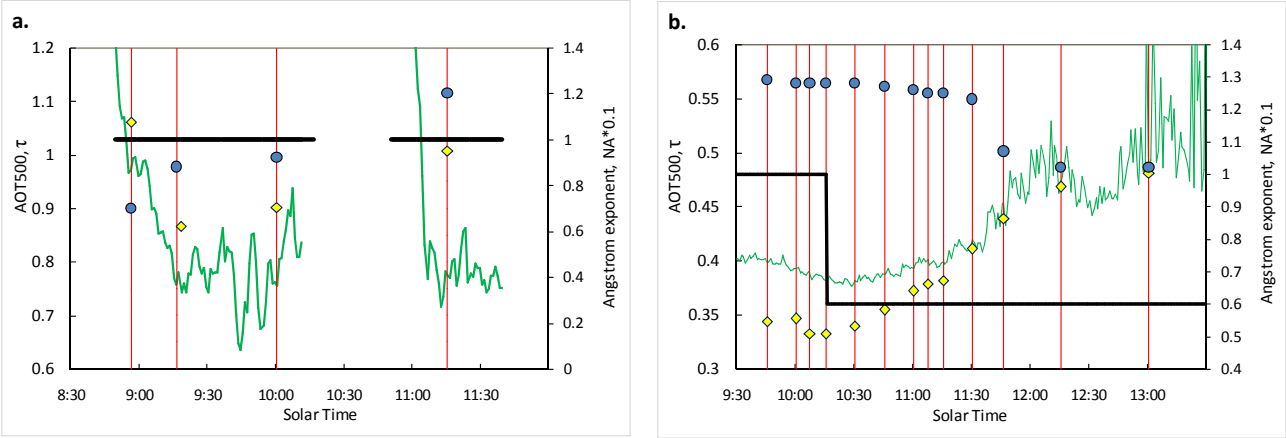

952

953

954

955 Fig.2. The time series in AOT500 (diamonds), integral optical thickness τ (green line), Angstrom
956 exponent (circles), and total cloud amount NA*0.1 (black lines) during February 27th, 2005 (a) and
957 February 1st, 2006 (b) in contaminated cloud conditions. Note, that τ is given only as an indicator of
958 aerosol/cloud stability conditions during the AERONET measurements. See further details in the text.

959

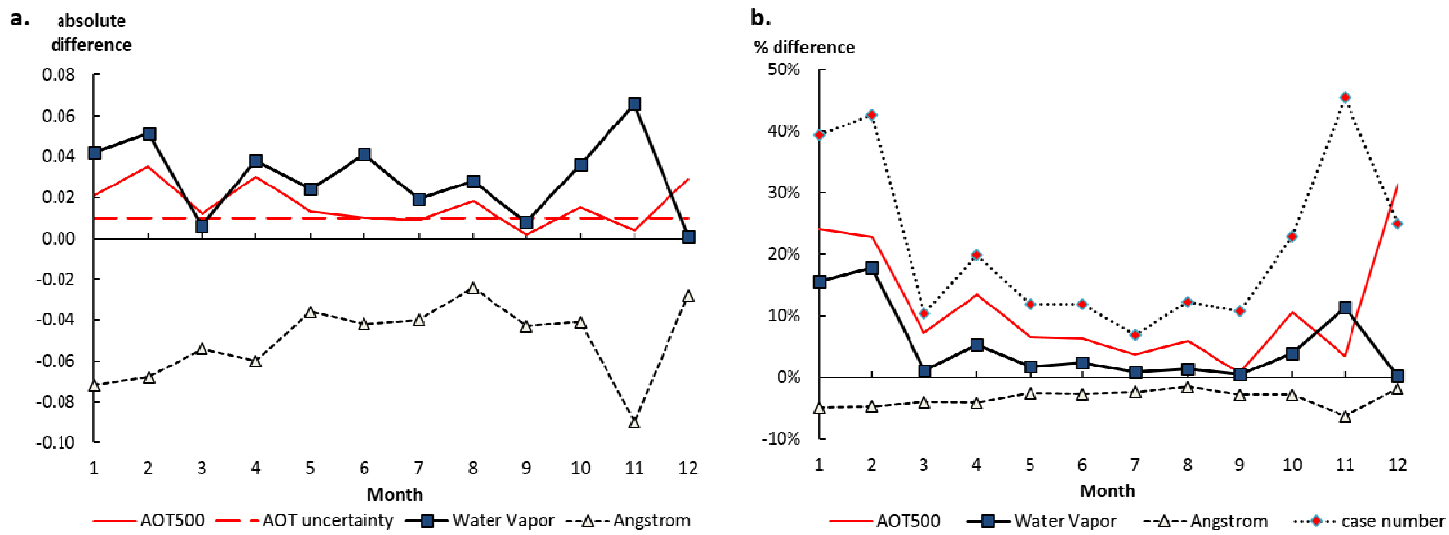

Fig.3. The absolute (a) and relative (b) difference of monthly mean standard level 2.0 data on aerosol optical thickness at 500nm (AOT500), Angstrom exponent and water vapour with the dataset after additional cloud correction. The standard uncertainty of AOT measurements is shown in Fig.2a. Relative changes in day number removed after additional cloud correction is shown in Fig2b. Moscow, 2001-2014 period. Note, that in Fig.2a the difference in water vapour is given in cm and other characteristics are dimensionless.

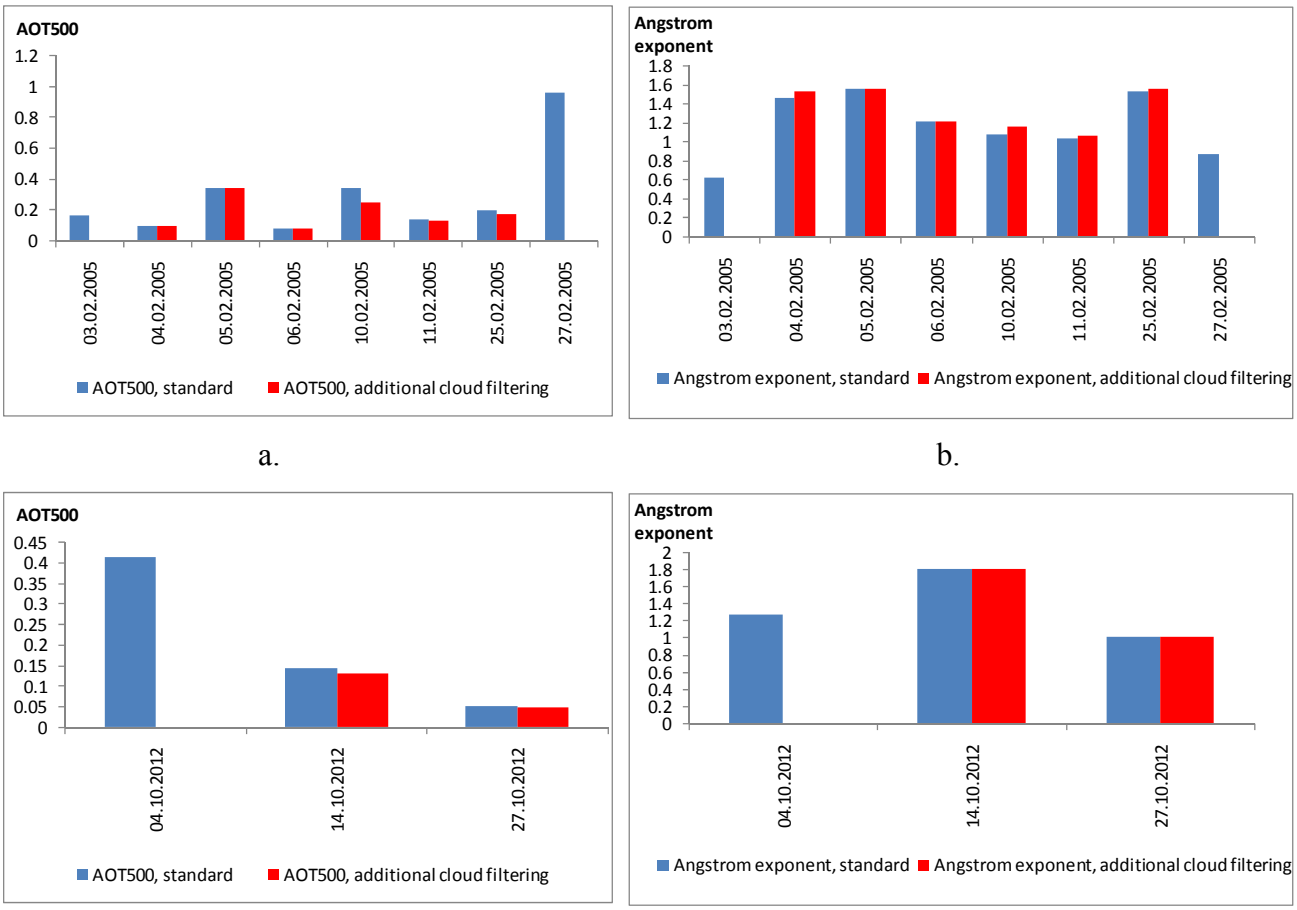

Fig.4. Standard AERONET AOT500 (a,c) and Angstrom exponent (b,d) daily means and their values after the application of the additional cloud screening for the months with large monthly mean AOT bias from the standard AERONET dataset (February, 2005(a,b), October, 2012(c,d)). Note, that the absence of the red columns (revised dataset) for several days means full elimination of the aerosol measurements after additional cloud checking. The solar disk was obscured by Cirrus, Cirrocumulus, Cirrostratus clouds during both days with SD=1, and SD=0. The halo was detected. See further description in the text.

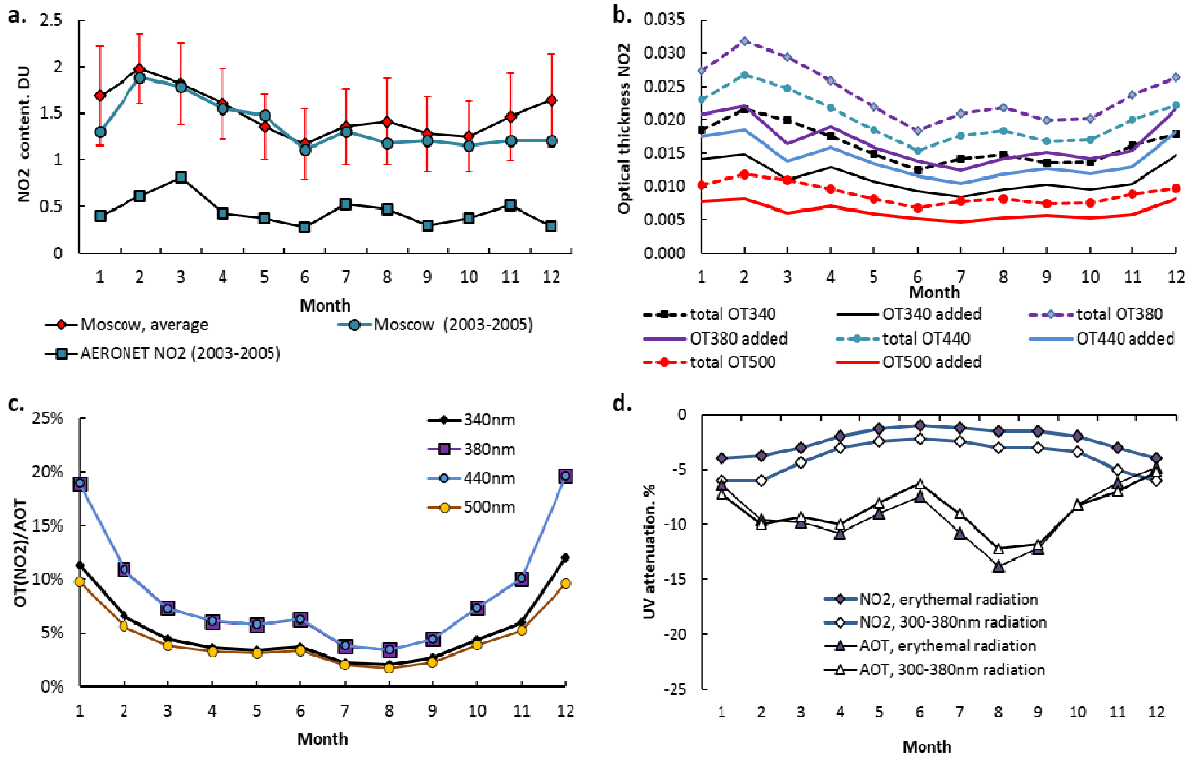

Fig.5. The seasonal distribution of mean NO_2 content over 2002-2013 and 2003-2005 periods obtained according to (Chubarova et al., 2010) and the NO_2 retrievals applied in the standard AERONET algorithm (a); monthly mean total and additional optical thickness (OT) of NO_2 at different wavelengths (b); monthly mean ratio $OT(NO_2)/AOT$ at different wavelengths (c); relative attenuation of erythemal radiation and UV radiation 300-380nm due to NO_2 and AOT at noon time conditions according to the results of 8-stream DISORT method (d). Moscow.

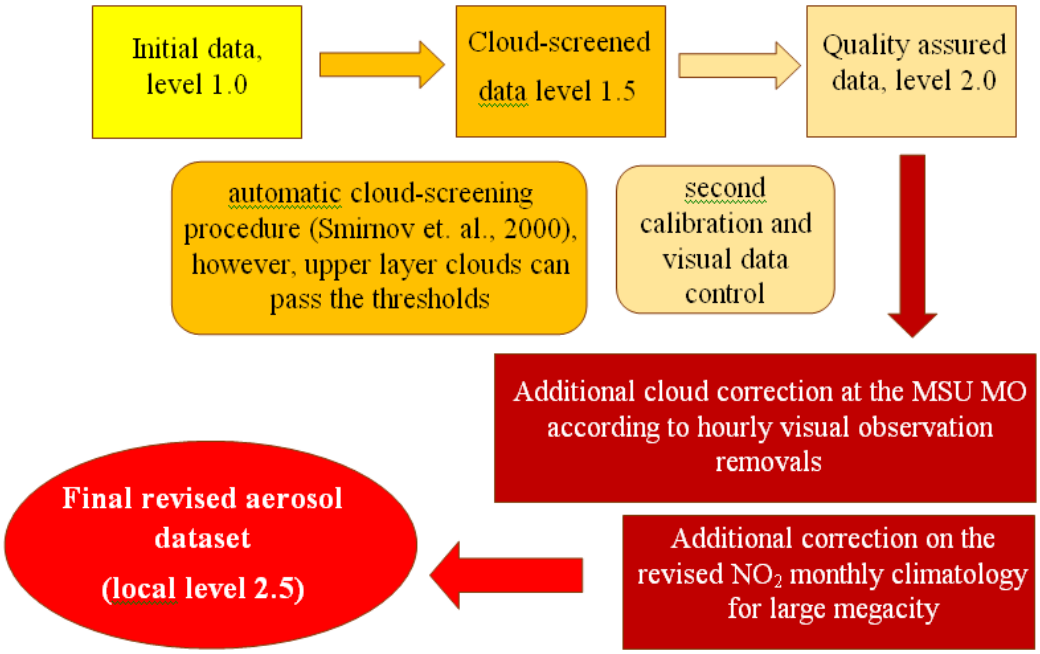

Fig.6. The scheme of the updated AERONET data proceeding with additional cloud and NO_2 correction used at the Moscow MSU MO.

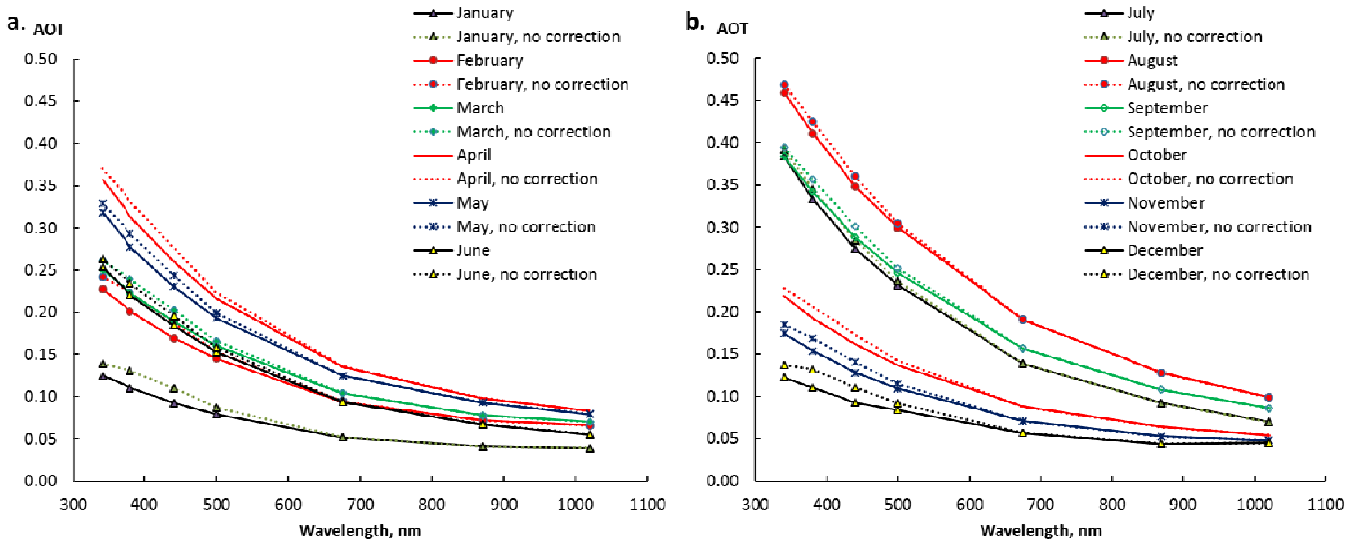

Fig.7. Spectral dependence of monthly mean AOT according to the standard and the revised AERONET dataset with the additional cloud and NO_2 correction. Moscow, 2001-2014 period.

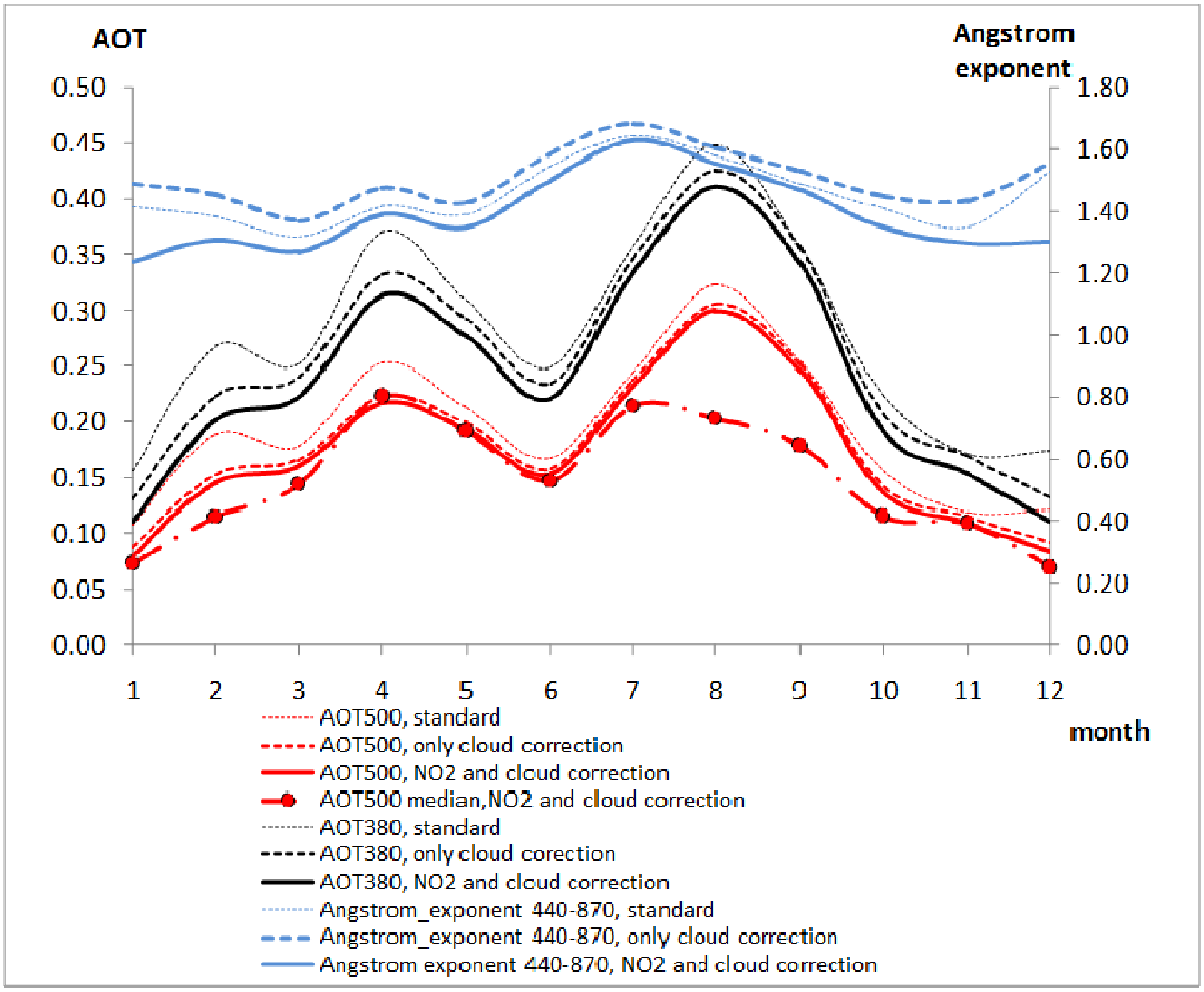

Fig.8. Seasonal variation of monthly mean aerosol optical thickness at 380 and 500 nm, median AOT at 500 nm, and Angstrom exponent according to the standard AERONET level 2.0 dataset, the data after additional cloud correction, and the final revised dataset. Note, that the additional correction of cloud and NO_2 has different sign for Angstrom exponent. Moscow, 2001-2014 period.

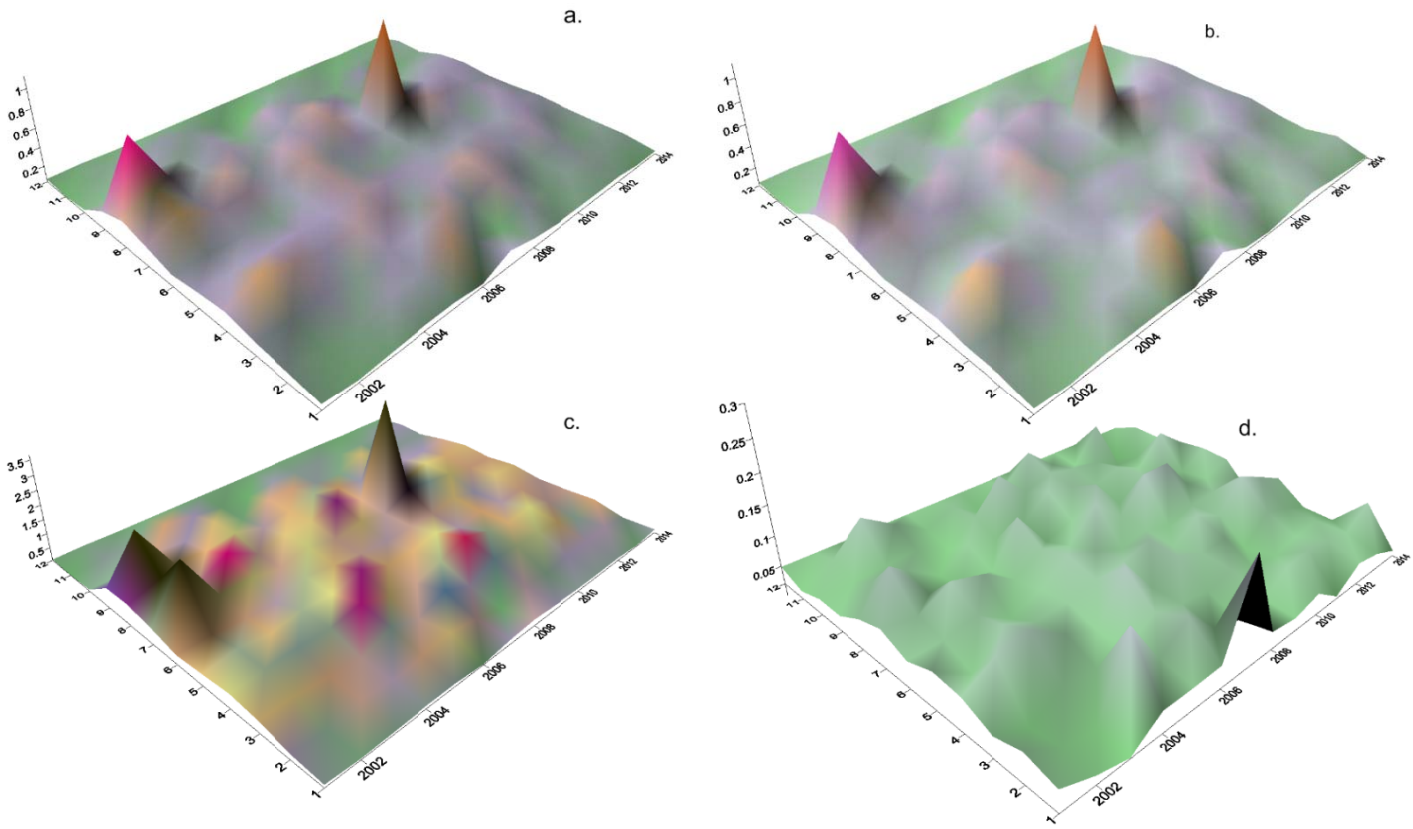

Fig.9. 3-D distribution of the revised monthly mean AOT500 (a), 50% quantile AOT500 (b), daily AOT500 maximum (c) and daily AOT500 minimum (d). Moscow.

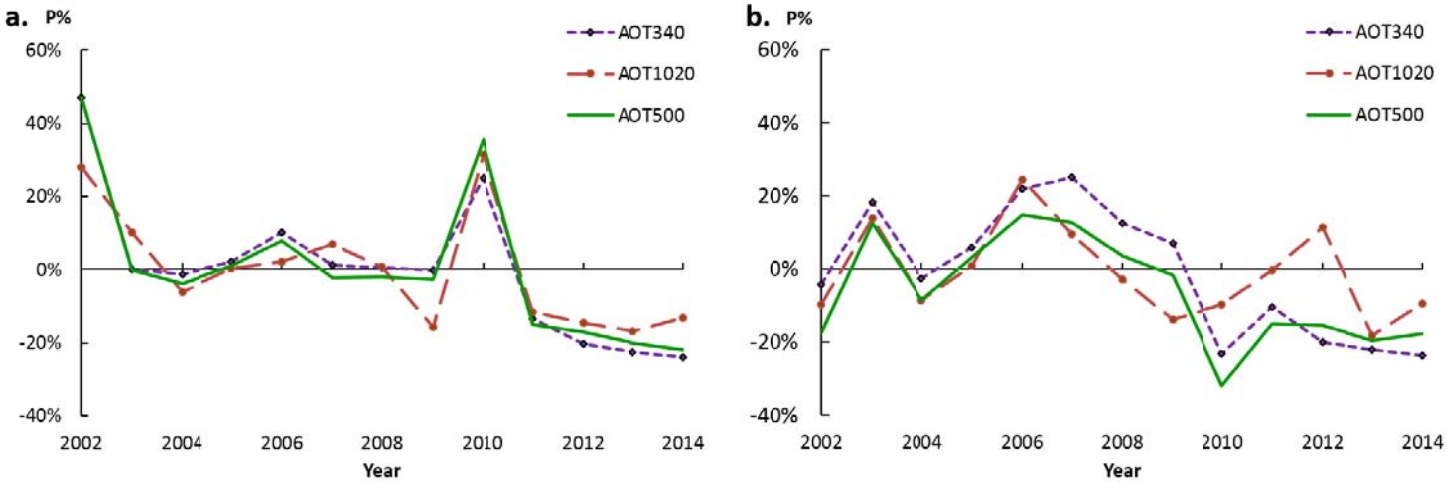

Fig.10. Interannual variations of the revised annual mean (a) and 50% quantile (b) AOT at several wavelengths. Moscow.

Comment: the annual 50% quantile AOT is estimated from monthly 50% quantile AOT values. For consistency the 2001 data were not used since the measurements have been in operation only from August.

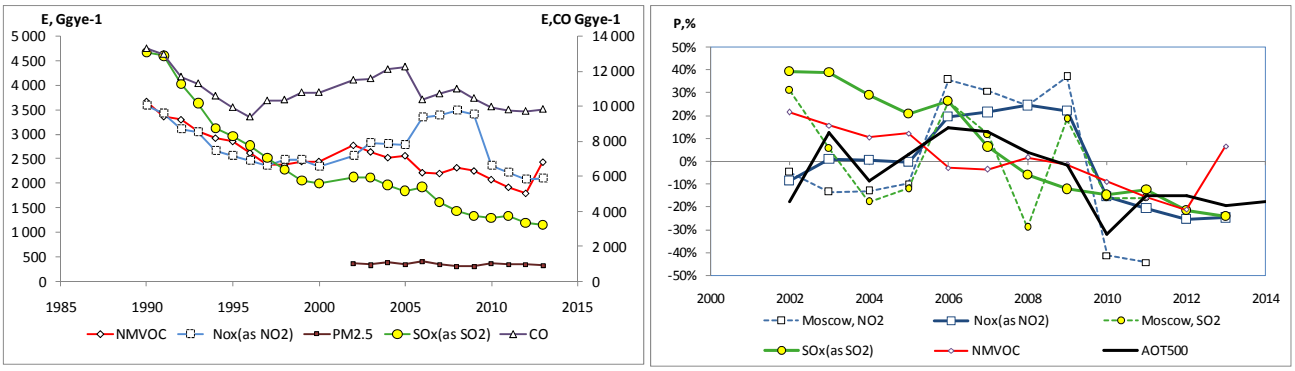

a. b.

Fig.11. Interannual variations in emissions of main aerosol precursors (SOx, NOx, NMVOC), CO, and particulate matter (PM2.5) according to WebDab - EMEP database over European part of Russia (a), relative changes in 50% quantile AOT500 and in SO_x and NO_x emissions over European part of Russia and directly over Moscow (b).

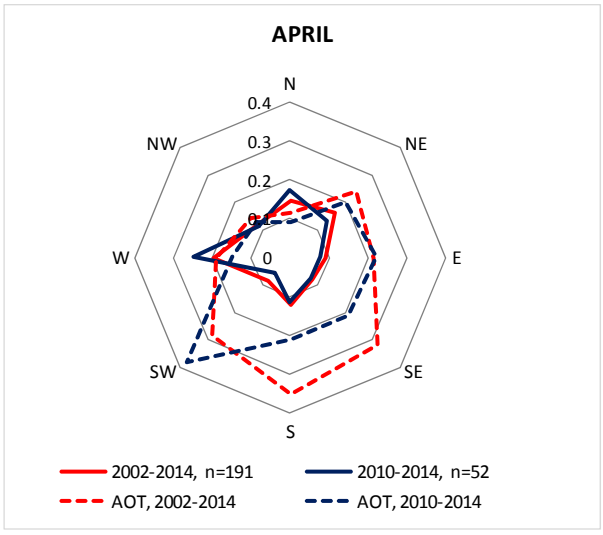

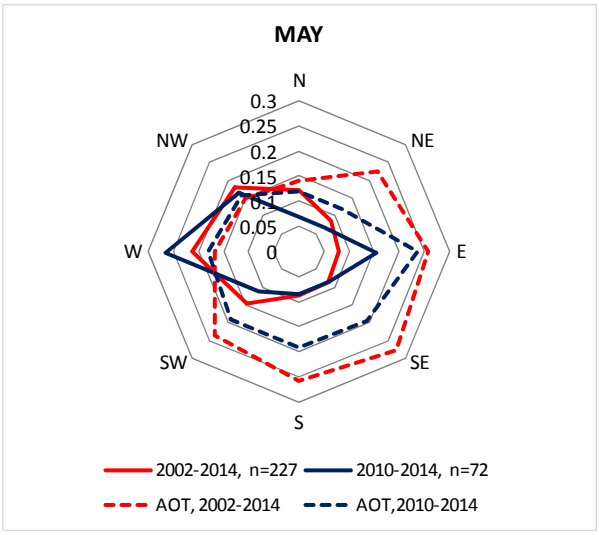

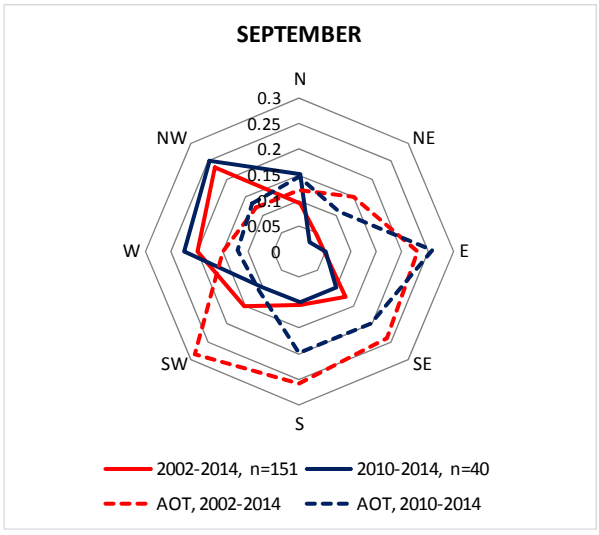

Fig.12. The wind diagram (in unit fraction) over the whole period of observations (2002-2014) and over the 2010-2014 period (solid lines) and distribution of AOT500 at different wind directions over the same periods (dashed line) (in AOT units) for the months with statistically significant negative trends. Wind directions were obtained according to the NOAA HYSPLIT model 24- hour backward trajectory analysis at 500m AGL for 12h UTC.

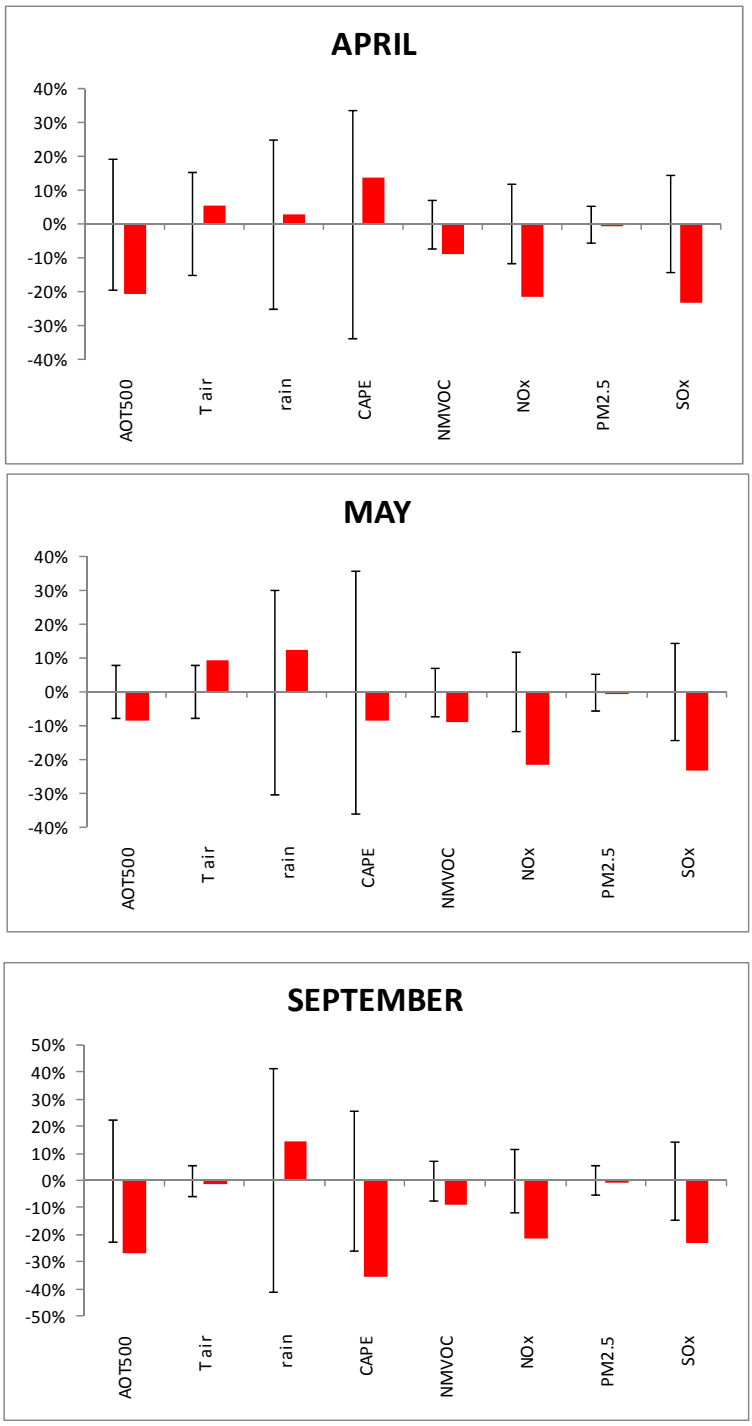

Fig.13. Error bars interval at confidence level P=95% of relatively change in monthly mean AOT500, air temperature (Tair), precipitation (rain), CAPE, as well as different emissions (NMVOC, NOx, PM2.5, SOx) from the WebDab – EMEP database and mean relative changes of these characteristics over 2010-2014. All the data were normalized against their mean values over the whole period of observation. For homogeneity reasons we do not include September 2002 in the analysis due to the large effect of smoke aerosol from forest fires, and April 2012, since it was a problem with sun photometer records. Note, that the emissions data are available only up to 2013.

FIGURE CAPTIONS

Fig.1. Mean aerosol optical thickness at 500nm (AOT500) and Angstrom exponent within 440-870 nm spectral range in different samples with various total cloud amount (NA) thresholds for the central months of the seasons. Moscow, 2001-2014. Number of days with measurements for each sample is given in brackets. Note, that the error bars are shown at the confidence level P=80%.

Fig.2. The time series in AOT500 (diamonds), integral optical thickness τ (green line), Angstrom exponentr (circles), and total cloud amount NA*0.1 (black lines) during February 27th, 2005 (a) and February 1st, 2006 (b) in contaminated cloud conditions. Note, that τ is given only as an indicator of aerosol/cloud stability conditions during the AERONET measurements. See further details in the text.

Fig.3. The absolute (a) and relative (b) difference of monthly mean standard level 2.0 data on aerosol optical thickness at 500nm (AOT500), Angstrom exponent and water vapour with the dataset after additional cloud correction. The standard uncertainty of AOT measurements is shown in Fig.2a. Relative changes in day number removed after additional cloud correction is shown in Fig2b. Moscow, 2001-2014 period. Note, that in Fig.2a the difference in water vapour is given in cm and other characteristics are dimensionless.

Fig.4. Standard AERONET AOT500 (a,c) and Angstrom exponent (b,d) daily means and their values after the application of the additional cloud screening for the months with large monthly mean AOT bias from the standard AERONET dataset (February, 2005(a,b), October, 2012(c,d)). Note, that the absence of the red columns (revised dataset) for several days means full elimination of the aerosol measurements after additional cloud checking. The solar disk was obscured by Cirrus, Cirrocumulus, Cirrostratus clouds during both days with SD=1, and SD=0. The halo was detected. See further description in the text.

Fig.5. The seasonal distribution of mean NO_2 content over 2002-2013 and 2003-2005 periods obtained according to (Chubarova et al., 2010) and the NO_2 retrievals applied in the standard AERONET algorithm (a); monthly mean total and additional optical thickness (OT) of NO_2 at different wavelengths (b); monthly mean ratio OT(NO_2)/AOT at different wavelengths (c); relative attenuation of erythemal radiation and UV radiation 300-380nm due to NO_2 and AOT at noon time conditions according to the results of 8-stream DISORT method (d). Moscow.

Fig.6. The scheme of the updated AERONET data proceeding with additional cloud and NO_2 correction used at the Moscow MSU MO.

Fig.7. Spectral dependence of monthly mean AOT according to the standard and the revised AERONET dataset with the additional cloud and NO_2 correction. Moscow, 2001-2014 period.

Fig.8. Seasonal variation of monthly mean aerosol optical thickness at 380 and 500 nm, median AOT at 500 nm, and Angstrom exponent according to the standard AERONET level 2.0 dataset, the data after additional cloud correction, and the final revised dataset. Note, that the additional correction of cloud and NO_2 has different sign for Angstrom exponent. Moscow, 2001-2014 period.

Fig.9. 3-D distribution of the revised monthly mean AOT500 (a), 50% quantile AOT500 (b), daily AOT500 maximum (c) and daily AOT500 minimum (d). Moscow.

Fig.10. Interannual variations of the revised annual mean (a) and 50% quantile (b) AOT at several wavelengths. Moscow.

Comment: the annual 50% quantile AOT is estimated from monthly 50% quantile AOT values. For consistency the 2001 data were not used since the measurements have been in operation only from August.

Fig.11. Interannual variations in emissions of main aerosol precursors (SOx, NOx, NMVOC), CO, and particulate matter (PM2.5) according to WebDab - EMEP database over European part of Russia (a), relative changes in 50% quantile AOT500 and in SO_x and NO_x emissions over European part of Russia and directly over Moscow (b).

Fig.12. The wind diagram (in unit fraction) over the whole period of observations (2002-2014) and over the 2010-2014 period (solid lines) and distribution of AOT500 at different wind directions over the same periods (dashed line) (in AOT units) for the months with statistically significant negative trends. Wind

1151 directions were obtained according to the NOAA HYSPLIT model 24- hour backward trajectory analysis
1152 at 500m AGL for 12h UTC.
1153
1154 Fig.13. Error bars interval at confidence level P=95% of relatively change in monthly mean AOT500, air
1155 temperature (Tair), precipitation (rain), CAPE, as well as different emissions (NMVOC, NOx, PM2.5,
1156 SOx) from the WebDab – EMEP database and mean relative changes of these characteristics over 2010-
1157 2014. All the data were normalized against their mean values over the whole period of observation. For
1158 homogeneity reasons we do not include September 2002 in the analysis due to the large effect of smoke
1159 aerosol from forest fires, and April 2012, since it was a problem with sun photometer records. Note, that
1160 the emissions data are available only up to 2013.
1161